Pathomechanism and therapeutic possibilities of mitochondrial dysfunction in ischemia-reperfusion

Gerda Strifler

Ph.D. Thesis

Institute of Surgical Research, University of Szeged
Szeged, Hungary

2016
Szeged

CONTENTS

List of abbreviations

Ama	antimycin A
As	ascorbate
ATP	adenosine triphosphate
CCCP	carbonyl cyanide m-chlorophenyl hydrazine
CH_4	methane
CLSEM	laser-scanning confocal microscopy
DAPI	4',6-diamidino-2-phenylindole staining
ETC	electron transport chain
ETS	electron transport system
G	glutamate
GI	gastrointestinal
GPC	L-alpha glycerylphosphorylcholine
GSH	reduced glutathione
GSSG	oxidized glutathione disulfide
H_2O_2	hydrogen peroxide
HRR	high-resolution respirometry
IL-1	interleukin-1
IR	ischemia-reperfusion
M	malate
MDA	malondialdehyde
MitOx	mitochondrial respiratory medium
MPO	myeloperoxidase
MSRs	methionine sulfoxide reductases
NADPH	nicotinamide adenine dinucleotide phosphate
NAFLDs	nonalcoholic fatty liver diseases
NOx	tissue nitrite/nitrate level
O_2	oxygen
O2k	Oxygraph-2k
Omy	oligomycin
OxPhos	oxidative phosphorylation
PC	phosphatidylcholine
PMN	polymorphonuclear leukocytes

RNS	reactive nitrogen species
ROS	reactive oxygen species
Rot	rotenone
S	succinate
SH	sham operated
SUIT	substrate-uncoupler-inhibitor titration
TMPD	N,N,N,N-tetramethyl-p-phenylenediamine
TNF-α	tumor necrosis factor-α
TUNEL	terminal deoxynucleotidyl transferase dUTP nick end labelling
XOR	xanthine oxidoreductase

List of original papers

List of full papers relating to the subject of the thesis

Strifler G, Tuboly E, Szél E, Kaszonyi E, Cao C, Kaszaki J, Mészáros A, Boros M, Hartmann P. Inhaled Methane limits the mitochondrial electron transport chain dysfunction during experimental liver ischemia-reperfusion injury. PLoS ONE 11:(1) Paper e0146363. (2016) **IF: 3,057***

Strifler G, Tuboly E, Görbe A, Boros M, Hartmann P. Targeting mitochondrial dysfunction with L-alpha glycerylphosphorylcholine. PLoS ONE 11(11):e0166682. (2016) **IF: 3,057***

Strifler G, Mészáros A, Pécz D, Ficzere Á, Baráth B, Boros M, Hartmann P. A májfunkció vizsgálata respirometriával. MAGYAR SEBÉSZET (accepted for publication)

Abstracts relating to the subject of the thesis

Strifler G, Tuboly E, Szél E, Kaszonyi E, Cao C, Kaszaki J, Mészáros A, Boros M, Hartmann P. Inhaled Methane limits the mitochondrial electron transport chain dysfunction during experimental liver ischemia-reperfusion injury. EUROPEAN SURGICAL RESEARCH 55:(Suppl. 1.) Paper OP-12. (2015)

Strifler G, Fehér Á, Kaszonyi E, Gowda A, Kaszaki J, Boros M, Hartmann P. Metánlélegeztetés májmitokondriumokra gyakorolt hatása részleges máj ischaemia-reperfúziós károsodásban patkányokban. MAGYAR SEBÉSZET 68:(3) p. 115. (2015)

Strifler G, Hartmann P, Mészáros A, Kaszonyi E, Cao C, Kaszaki J, Boros M. Effects of methane inhalation on rat liver mitochondria following partial hepatic ischemia. ACTA PHYSIOLOGICA 211:(S697) p. 170. (2014)

List of full papers not-relating to the subject of the thesis

Szalai Z, Szász A, Nagy I, Puskás LG, Kupai K, Király A, Magyariné Berkó A, Pósa A, **Strifler G,** Baráth Z, Nagy LI, Szabó R, Pávó I, Murlasits Z, Gyöngyösi M, Varga C. Anti-inflammatory effect of recreational exercise in TNBS induced colitis in rats: role of

NOS/HO/MPO system. OXIDATIVE MEDICINE AND CELLULAR LONGEVITY 2014: Paper 925981. 11 p. (2014) **IF: 3,516**

Szasz A, **Strifler G,** Voros A, Vaczi B, Tubak V, Puskas LG, Belso N, Kemeny L, Nagy I. The expression of TAM receptors and their ligand Gas6 is downregulated in psoriasis. JOURNAL OF DERMATOLOGICAL SCIENCE 71:(3) pp. 215-216. (2013) **IF: 3,335**

Cumulative IF: 12,965

1. INTRODUCTION

1.1. Mitochondria, structure and function

Mitochondria are membrane-enclosed organelles, they are the energy-producing centers in eukaryotic cells. The inner mitochondrial membrane is loaded with the protein complexes of the electron transport chain (ETC) and adenosine triphosphate (ATP) synthesis. This membrane surrounds the matrix, in which the citric acid cycle produces the electrons that enter and skip through the ETC. The outer membrane has many protein-based pores that allow the passage of ions and molecules as large as a small protein. In contrast, the permeability of the inner membrane is more restricted than that of the cell membrane. Mitochondria produce ATP during oxidative phosphorylation, control the oxidative state of the cell, and are major regulators of caspase-dependent and caspase-independent apoptotic pathways. Mitochondria are also involved in other cellular activities like signaling, differentiation, senescence, and the control of cell cycle and growth. The number of mitochondria in a cell can vary widely depending on the organism, tissue or cell type. For example, red blood cells have no mitochondria, whereas liver cells can have more than 2000 (Alberts 1994).

1.1.2. The mitochondrial electron transport

Electrons are transported through the complexes of the ETC, and are finally accepted by an oxygen molecule. This process drives the ATP synthesis, the exclusive source of cellular energy (Figure 1). The electrons enter the ETC at complex I, the nicotinamide adenine dinucleotide (NADH) dehydrogenase, and then skip to coenzyme Q. From coenzyme Q, the electrons are passed to complex III, the cytochrome c reductase, which is associated with another proton translocation event. The electrons flow from complex III to cytochrome c, and then to complex IV, the cytochrome oxidase complex. Electrons accumulate at complex IV, the end complex of ETC, where the protons and the electrons are finally accepted by oxygen molecules. As a result, the oxygen is reduced to water; meanwhile the proton gradient generates the proton motive force for ATP synthase. Complex II, the succinate dehydrogenase complex, is a separate starting point, where the electrons can enter from succinate and flow back to coenzyme Q, and then again to complex III, cytochrome c and complex IV. Thus, there is a common electron transport pathway beyond the two entry points, either complex I or complex II, and a reverse electron flow

step between them. In summary, substrate oxidation by the ETC creates a proton gradient across the inner membrane, and for optimal performance, the electron shuttle must be in a steady state as regards the two entry points and the final utilization points. Oxygen availability, is therefore crucial.

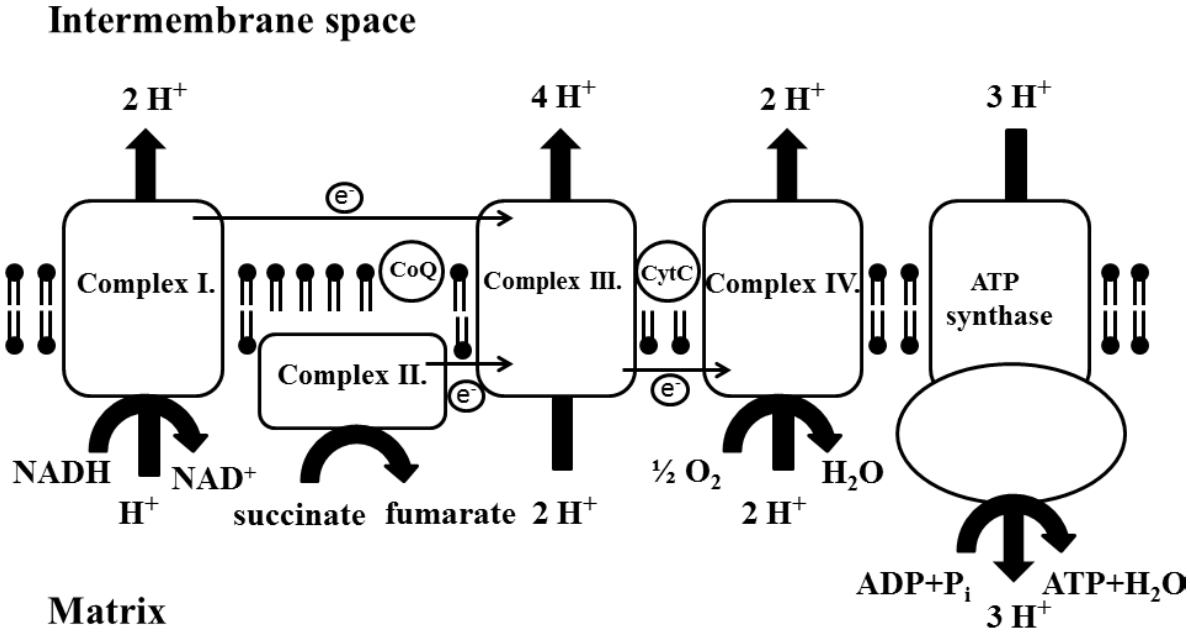

Figure 1. The mitochondrial electron transport chain

1.2. Mitochondrial dysfunction in liver diseases

Due to their diverse physiological functions, dysfunctional mitochondria can cause various acute and chronic diseases, thus being potential targets for therapies and diagnostics. Liver diseases are also often accompanied by mitochondrial functional disorders, and likewise, diseases of the mitochondria can cause damage to liver cells. Hepatic manifestations of mitochondrial disorders range from steatosis, fibrosis and cirrhosis to hepatocellular carcinoma and chronic liver failure (Pessayre 2005; Caldwell 1999; Sanyal 2001; Ibdah 2005). These conditions belong to a group of non-alcoholic fatty liver diseases (NAFLDs) which have a high prevalence worldwide (Clark 2002). The NAFLD-associated mitochondrial defects include reduced activity of respiratory chain complexes and decreased mitochondrial β-oxidation. Ultrastructural lesions, such as swelling, paracrystalline inclusions in the matrix and hypodensity have also been shown by electron microscopy (Wei 2008). Mitochondria play a central role in changes in liver architecture as well, because they can mediate death receptor signaling, metabolic disorders and fibrosis. As an end-stage of NAFLDs, hepatocellular carcinoma is the most common

malignant tumor of the liver. Mitochondrial dysfunctions in hepatocellular carcinoma display increased ROS production, Ca^{2+}mobilization and reduced ATP generation (Chang 2009).

1.2.1 Ischemia-reperfusion (IR)-induced mitochondrial disturbances

IR injury is a common complication of inflow-controlled major surgical resections and organ transplantations. The main source of reactive oxygen species (ROS) in hepatic IR injury are the mitochondria of activated sinusoidal endothelial cells and hepatocytes (Kalashnyk 2012). The lack of oxygen during ischemia causes a decrease in ATP production, and an increase in ATP hydrolysis due to the subsequent activation of anaerobic metabolism. In contrast, restoration of the blood flow during the reoxygenation phase leads to overproduction of superoxide, mainly at the sites of complexes I and III (Kalashnyk 2012). Loss of calcium homeostasis, production of ROS and ETC damage are all different aspects of mitochondria-related changes in IR (Hines 2003).

ROS can also derive from xanthine dehydrogenase/xanthine oxidase (XOR) system, furthermore, infiltrating polymorphonuclear leukocytes (PMNs) also produce ROS and cytokines upon reperfusion (Granger 1986; Schoenberg 1991; Lojek 1997). Cytokines promote the recruitment of PMNs and the expression of myeloperoxidase (MPO) enzyme upon their activation, thereby contributing to the progression of parenchymal injury. These cytokines amplify Kupffer cell activation, tumor necrosis factor-α (TNF-α) and interleukin-1 (IL-1) secretion, and promote PMN recruitment and sticking into the liver sinusoids. In addition to high level ROS generation, liver IR injury leads to lower levels of antioxidants such as glutathione (GSH) or superoxide dismutase.

Mitochondria are not only sources but also target organelles of IR-related intracellular changes; hence ischemia impairs both their structural and functional integrity. Lipid peroxidation, corresponding to the peroxidation of polyunsaturated fatty acids, is a well-known consequence of IR injury. The degree of lipid peroxidation can be estimated via the amount of malondialdehyde (MDA), a marker of oxidative damage of membranes. In fact, the overproduction of ROS during the reperfusion phase results in oxidative damage and mitochondrial inner membrane permeability transition (Hirakawa 2003). In the case of elevated membrane permeability, cytochrome c is released in considerable amounts as major starting molecules of apoptosis. Cytochrome c activates caspases 3, the point of no return of the apoptosis pathway, thus lipid peroxidation inevitably induces apoptosis. Furthermore, caspase 3 activates other effective caspases as well, leading to substrate

proteolysis (structure proteins, cell cycle proteins). The caspase-dependent apoptotic pathway is actively regulated, which means that ATP is required to proceed. Consequently, when ATP level decreases in IR conditions, cell necrosis occurs more frequently, which is a passive, ATP-independent way of cell death.

1.3. Examination of mitochondrial functions with high-resolution respirometry

Respirometry detects the consumption of oxygen and it is the main tool to study mitochondrial function (Gnaiger 2000). In recent years, high-resolution respirometers have been developed which allow to determine many parameters of mitochondrial function in routine assays using small samples of biological material. The Oxygraph-2k (Oroboros Instruments, Innsbruck; Austria) is a second generation respirometer (Figure 2), equipped with two experimental chambers in which mitochondria, living cells or freshly prepared tissue samples are suspended in a suitable medium. Each chamber is supplied with an oxygen sensor and the oxygen consumption of mitochondria can be computed based on the changes in oxygen concentration in the chambers. Three different types of samples may be subjected to respirometric studies: isolated mitochondria, permeabilized cells and permeabilized tissues (e.g. precisely cut liver samples). In the latter cases the cellular membrane is made permeable in order to facilitate chemicals to cross over the membrane. During the respirometric measurements, the mitochondria undergo different “states” by the sequential addition of substrates or inhibitors (Figure 3). The key advantage of this approach is that the respiratory capacity can be assessed at multiple levels of the respiratory chain which makes the technique a powerful tool for studying the complex mitochodrial functionality. There are many possible human fields of application in conditions and diseases where a linkage to mitochondria is expected, such as diabetes mellitus type 2 (Jelenik 2013), obesity (Schöttl 2015), IR injuries (Gnaiger 2001), aging and cancer (Domenis 2011).

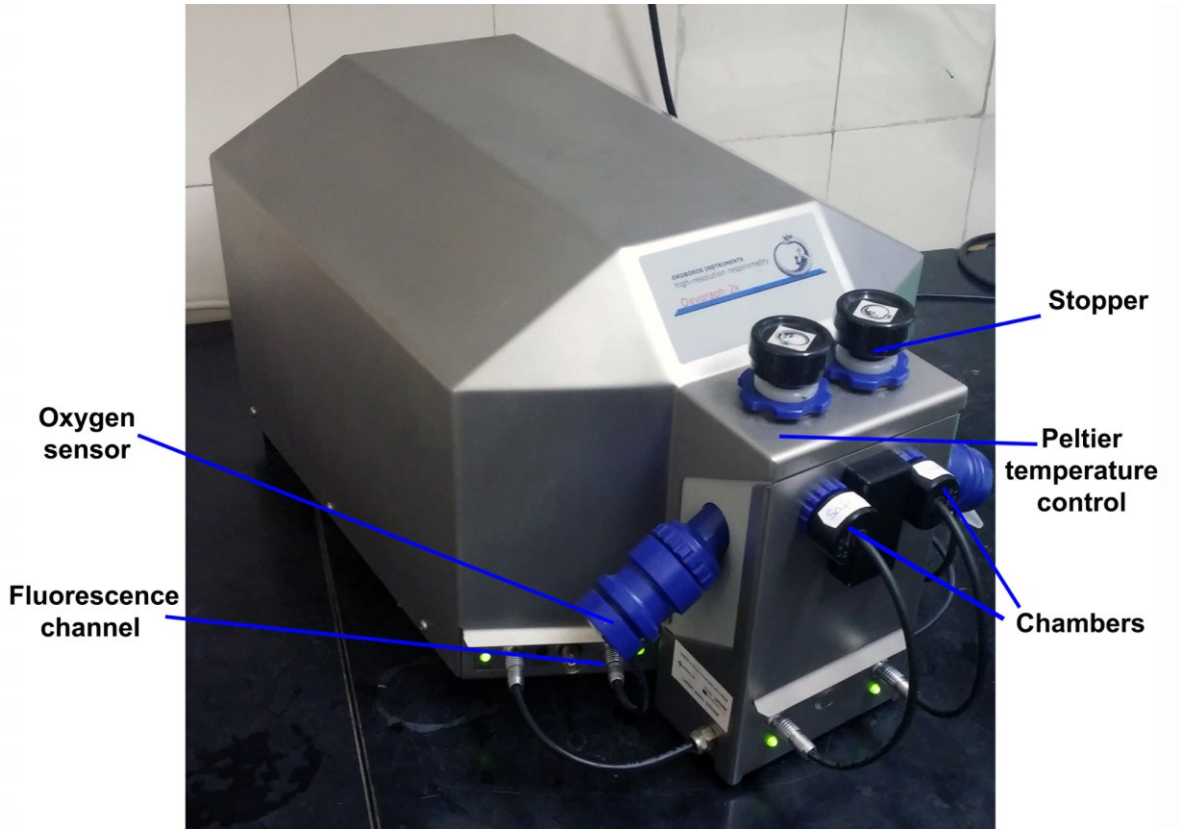

Figure 2. The Oxygraph-2k high-resolution respirometer

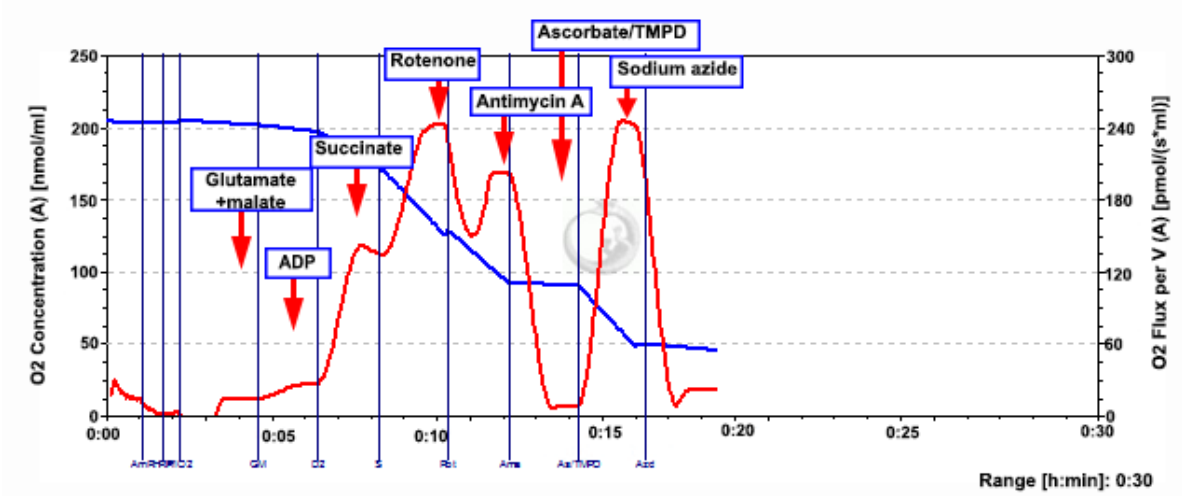

Figure 3. To measure the respiratory activity of the liver mitochondria, tissue samples are homogenized in mitochondrial respiration medium and then subjected to high-resolution respirometry. Glutamate (2 mM) and malate (10 mM) were used in combination to induce complex I-linked respiration. The complex II-linked state II respiration was determined with 10 mM succinate, saturating ADP (2.5 mM final concentration) was added in order to stimulate respiration to the level of OxPhos capacity. Complex I was inhibited by rotenone (0.5 µM) and complex III by antimycin A (2.5 µM). Finally, 2 mM ascorbate and 20 µM *N,N,N,N*-tetramethyl-*p*-phenylenediamine (TMPD) were added for complex IV-linked respiration, which was inhibited by sodium azide (50 mM).

1.4. Bioactivity of methane (CH_4)

CH_4 is the simplest alkane and the main component of natural gas environment. At room temperature and at atmospheric pressure, CH_4 is a colorless, odorless gas. It plays a well-known role in tropospheric and stratospheric chemistry, where the mass of the released CH_4 is oxidized to carbon dioxide due to its reactivity with hydroxyl radicals (Cantrell, 1990; Hurkuck, 2012). The atmospheric CH_4 concentration has been increased approximately 2.5-fold since preindustrial times, and it is therefore regarded as a significant greenhouse gas of growing ecological importance (Denman, 2007; Mitchell, 2013). Naturally-occurring CH_4 is mainly produced by methanogenesis. This multistep process is used by microorganisms as an energy source (Hamilton 2003).

CH_4 is intrinsically nontoxic *in vivo*. It is a simple asphyxiant, which means that tissue hypoxia may occur when CH_4 displaces air, and hence oxygen, in a restricted space, and the concentration of oxygen is reduced to below approximately 18% in the internal milieu of the body. Nevertheless, the inhalation of normoxic air containing 2.5% CH_4 for 3 hours has been shown to have no side-effects on the blood gas chemistry, and not to influence the macrohemodynamics in unstressed animals (Boros 2012). On the other hand, CH_4 can readily change the symbiosis with other gas molecules in closed spaces. The details and consequences of such *in vivo* relationships are basically unknown because determination of the intracellular distribution of these gas molecules is technically limited.

1.4.1. Mitochondria might be intracellular targets of CH_4

Mammalian methanogenesis is widely regarded as an indicator of the gastrointestinal (GI) carbohydrate fermentation by the anaerobic flora. Once generated by microbes or released by a nonbacterial process, CH_4 is generally considered to be biologically inactive. However, some data do hint at an association with the small bowel motility regulation, as CH_4 produced in the GI tract is usually associated with a decreased intestinal transit time, and other results suggest that CH_4 production (usually defined as a > 1 ppm elevation of exhaled CH_4 over the atmospheric level on breath testing) correlates with constipation in irritable bowel syndrome (Pimentel 2014). Information on the effects of exogenous CH_4 is sparse, but a previous study demonstrated that CH_4 supplementation can attenuate microcirculatory failure and the tissue accumulation of inflammatory cells in a large animal model of intestinal IR (Boros 2012). These data point to an anti-inflammatory potential for CH_4, but the identification of intracellular targets remains elusive (Boros 2012).

We postulated that, as they are critically involved in hypoxia-reoxygenation-induced intracellular respiratory damage, mitochondria may be targets of CH_4 administration. In particular, we hypothesized that if CH_4 is bioactive, it can exert its effect by influencing the respiratory activity and ROS production of mitochondria.

1.5. Biological and anti-inflammatory effects of L-alpha glycerylphosphorylcholine (GPC)

GPC is a water-soluble deacylated metabolite of phosphatidylcholine (PC) (Brownawell 2011), a source of choline and a precursor of acetylcholine (Abbiati 1993; Parnetti 2001). Under physiological conditions, GPC can be involved in the preservation of the structural integrity of cellular membranes, probably through the stimulation of PC synthesis via the Kennedy pathway (Gibellini 2010).

Moreover, it is also recognized that choline is used for CH_4 generation in various models of hypoxia and reoxygenation (in isolated mitochondria, endothelial cell cultures, in the exhaled air after reoxygenization of hypoxic animal tissues and in plants in response to excess excitation energy) (Ghyczy 2008). Today, the anti-inflammatory potential of choline is well established, but the underlying mechanism is not fully understood. Recently, it has been demonstrated that choline could participate in the "cholinergic anti-inflammatory pathway", including interference with the mechanism of activation of leukocytes or macrophages (Tracey 2000). Additionally, we have shown that exogenous PC increases tolerance to ischemia and hypoxia, and inhibits leukocyte accumulation in various experimental scenarios (Erős 2006, Hartmann 2009). We have also shown that CH_4-producing phospholipid substrates inhibit the formation of ROS proportional to the amount of CH_4 generated and the number of methyl groups in the molecules (Ghyczy 2008). It is especially notable that liver concentrations of endogenous GPC are significantly depleted after hemorrhagic shock, a prototype of systemic IR injury (Scribner 2010), and previous data suggest that exogenous GPC may influence tissue reactions in IR injury (Tőkés 2015; Hartmann 2014; Ghyczy 2008). Thus, the possible anti-inflammatory and scavenging potential of GPC is of particular importance, because it could offer means of targeting the inflammatory cascade without the confounding effects of mediators deriving from the metabolism of lipid side-chains.

1.5.1. Potential effects of GPC on mitochondria

Interestingly, mitochondrial inhibitors of the oxidative phosphorylation (OxPhos)

system can directly increase PC breakdown by activating phospholipase A_2, leading to an increased concentration of metabolic products (Farber 2000). It has also been demonstrated that membrane PC is depleted after an IR insult, and the liberated choline can play a protective role in the intracellular redox imbalance (Bruhl 2004). Furthermore, it was also shown that hepatic concentrations of GPC are significantly reduced after a period of hemorrhagic shock, with recovery to the baseline only 48 h later (Scribner 2010).

From therapeutic aspects, influencing mitochondrial damage is an appropriate strategy in hypoxia- or IR-related conditions, and the above indirect evidences all suggest that GPC may be an active and efficient compound in these settings. Based on this hypothesis, we plan to design *in vitro* tests using intact liver mitochondria in order to analyze the effects of GPC on mitochondrial function and on hypoxia-induced dysfunction. Following that, we intend to investigate the *in vivo* functional changes of liver mitochondria in response to a standardized IR challenge.

2. MAIN GOALS OF THE STUDIES

- The primary goal of the study was to characterize the functional changes of liver mitochondria in response to IR by means of high resolution respirometry.
  - First, we designed *in vitro* tests using intact liver mitochondria to study mitochondrial functions directly.
  - Furthermore, we planned to investigate mitochondrial ETC changes in unstressed animals or after a standardized IR insult.

- Secondly, we set out to investigate the effects of potentially effective treatments on IR-damaged hepatic mitochondria.

  - We hypothesized that inhaled CH_4 can influence the mitochondrial respiratory activity.
  - We hypothesized that the protective mechanism of exogenous GPC is also linked to mitochondria.

- Thirdly, we set out to investigate the mechanism of action of inhaled CH_4 and GPC treatments. We hypothesized that these pathways will interfere with ROS generation caused by ETC dysfunction, and thus pro-inflammatory cellular activation can be reduced.

3. MATERIALS AND METHODS

The experiments were carried out on male Sprague-Dawley rats (average weight 300±20 g, 7-8 weeks old) housed in an environmentally controlled room with a 12-hour light-dark cycle, and kept on commercial rat chow (Standard rat chow LT/n; Innovo Kft, Gödöllő, Hungary) and tap water *ad libitum*. The experimental protocol was in accordance with EU directive 2010/63 for the protection of animals used for scientific purposes, and it was approved by the National Scientific Ethical Committee on Animal Experimentation (National Competent Authority) with the license number V./148/2013. This study also complied with the criteria of the US National Institutes of Health Guidelines for the Care and Use of Laboratory Animals.

3.1. Surgical procedures

The rats were anesthetized with sodium pentobarbital (45 mg/kg ip), and the trachea was cannulated to facilitate respiration. The right jugular vein and carotid artery were cannulated for fluid and drug administration, respectively. Then small supplementary doses of pentobarbital were given intravenously (iv) when necessary. The animals were placed in a supine position on a heating pad to maintain the body temperature between 36 and 37 ºC, and Ringer's lactate was infused at a rate of 10 ml /kg/h during the experiments. For the preparation of the liver, the fur covering the abdomen was shaved, and the skin was disinfected with povidone iodide. After midline laparotomy and bilateral subcostal incisions, the liver was carefully mobilized from all ligamentous attachments. Complete ischemia of the median and left hepatic lobes was achieved by clamping the left lateral branches of the hepatic artery and the portal vein with a microsurgical clip for 60 min. After the period of ischemia, the clips were removed and measurements were performed during a 60-min reperfusion period (Hartmann 2014). The wound was temporarily covered with non-water-permeable foil during the reperfusion period.

3.2. Experimental protocols

3.2.1. Experimental series to study IR-induced changes in mitochondrial functions

The animals were randomly assigned to two groups. In the IR group (n=6), the rats were subjected to a 60-min complete ischemia followed by a 60-min reperfusion. Sham-operated animals (SH group, n=6) underwent the same surgical procedure but liver

ischemia was not induced. Liver samples were taken from the affected lobes at the end of the reperfusion period and at identical time point from the sham-operated animals.

3.2.2. Experimental series to study the effects of CH_4 on liver mitochondria

The animals were randomly assigned to one or another of the following groups. In the IR group (n=6), the mitochondrial respiratory functions in response to 60-min complete ischemia and 60-min reperfusion with normoxic air were examined. Control tissue samples were taken to determine the baseline mitochondrial respiratory variables, then ischemia was induced in the median and left hepatic lobes by clamping the left lateral branches of the hepatic artery and the portal vein. At 55 min of ischemia, liver samples were taken to analyze the mitochondrial respiration in response to ischemia. Following the release of the vascular occlusions, biopsies were obtained from the affected lobes at 5, 30 and 60 min of reperfusion. In the IR+CH_4 group (n=6), the protocol was identical, and additionally, inhalation with normoxic artificial air containing 2.2% CH_4 (Linde Gas, Budapest, Hungary) was started after 50 min of ischemia which continued throughout the reperfusion period. The sham-operated animals in the SH group (n=6) underwent the same surgical procedure but liver ischemia was not induced and the animals inhaled normoxic air, while the sham-operated animals in the SH+CH_4 group (n=6) were not subjected to liver ischemia, but inhaled CH_4 for the same duration as in the IR+CH_4 group.

3.2.3. Experimental series to study the effects of GPC on mitochondrial dysfunction-caused ROS generation

The animals were randomly assigned to four groups. In the vehicle-treated IR group (n=6), the rats were subjected to 60-min complete ischemia which was followed by 60-min reperfusion. In the IR+GPC group 16.56 mg/kg bw GPC (MW: 257.2, Lipoid GmbH, Ludwigshafen, Germany; dissolved in 0.5 ml of sterile saline solution at 0.064 mM concentration) was injected iv and the same protocol was used 5 min before the end of ischemia (Tőkés 2015). The sham-operated, vehicle-treated animals (SH group, n=6) underwent the same surgical procedure without liver ischemia, while another control group (SH+GPC group, n=6) received GPC in the same time-frame as the IR+GPC group.

3.3. High-resolution respirometry

Intact liver mitochondria from sham-operated animals were used to study *in vitro* mitochondrial functions directly. The isolation protocol was performed by the method of

Gnaiger et al. (Gneiger 2000). Briefly, mitochondria were isolated from the left liver lobe in isotonic sucrose medium (300 mM sucrose, 0.2 mM EDTA and 10 mM HEPES, adjusted to pH 7.4 with KOH at 4 °C). After the last centrifugation, mitochondrial pellets were resuspended in sucrose medium.

For the *in vivo* experiments, liver biopsy samples were taken at different time points of the experimental protocols. To determine the respiratory activity in the liver mitochondria, liver samples were homogenized in 1 ml of MitOx respiration medium with a glass Potter homogenizer, then 50 µl of homogenates were weighed into the detection chambers and subjected to high-resolution respirometry.

3.3.1. The Substrate-Uncoupler-Inhibitor Titration (SUIT) protocol to study IR-induced changes

The SUIT protocol was employed in liver homogenates to explore the IR-related changes in the electron transport system (ETS). Glutamate (2 mM) and malate (10 mM) were used in combination to induce complex I-linked respiration; saturating ADP (2.5 mM final concentration) was added in order to stimulate respiration to the level of OxPhos capacity. By adding succinate (10 mM), the complex I+complex II OxPhos capacity was detected, then the uncoupler carbonyl cyanide m-chlorophenyl hydrazine (CCCP) (C; 0.5 µM per step) was titrated. Finally, complex I was inhibited by rotenone (0.5 µM) and complex III by antimycin A (2.5 µM).

3.3.2. Effects of CH_4 on mitochondrial respiration

1. Pilot experiments were conducted to detect the changes in respiratory activity of different mitochondrial OxPhos system complexes in response to CH_4 in intact mitochondria. For respirometric analysis, isolated mitochondria were suspended in 1 ml MitOx medium and weighed into the chambers, while the gas phase contained the 2.2% CH_4-air mixture or room air (n=8). The rate of respiration was determined after the addition of 2 mM malate and 10 mM glutamate for complex I-linked respiration, 2.5 mM ADP for complex I state III respiration, 10 mM succinate for complex I and complex II state III respiration, 0.5 µM rotenone for complex II-linked respiration and finally 2.5 µM antimycin A, 2 mM ascorbate and 20 µM N,N,N,N-tetramethyl-p-phenylenediamine (TMPD) for complex IV-linked respiration.

2. Basal protocol was employed to study the ETS (state II) and OxPhos (state III) capacity of mitochondria (state II-III respiration protocol) from liver homogenates. The

steady-state oxygen consumption (respiratory flux) was observed; then, the complex II-linked state II respiration rate was determined with 10 mM succinate after the addition of 0.5 μM complex I inhibitor rotenone. To determine the maximum respiratory capacity of complex II-linked (state III) respiration, 2.5 mM ADP was added to the chamber. Finally, the intactness of the outer mitochondrial membrane was assessed after 10 μM cytochrome c addition. The respirometry data were normalized to wet weight (Hutter 2007).

3.3.3. Determination of the effective GPC concentration on mitochondrial functions

1. We have performed *in vitro* experiments to detect the changes in the respiratory activity of intact liver mitochondria in response to 30-min anoxia, with or without GPC administration, using high-resolution respirometry. In this experimental series, the animals were anesthetized for sample taking using sodium pentobarbital (45 mg/kg ip). The liver samples were weighed into the detection chambers, 50 μl in each, which were calibrated to 200 nmol/ml oxygen concentration in room air. In order to determine the effective GPC concentration range, series of GPC solutions from 1 nM to 800 mM were used. The steady-state basal oxygen consumption of the homogenates (respiratory flux) was measured. The complex II-linked state II respiration rate was then determined with 10 mM succinate after the addition of 0.5 μM complex I inhibitor rotenone. Then the complex II-linked (state III respiration) maximum respiratory capacity was estimated by adding saturating concentration of ADP to the medium. Subsequently, anoxia was applied and, at the end of the 30-min anoxic period, the chambers were opened to recover the mitochondria at 200 nmol/ml oxygen concentration.

2. The SUIT protocol was employed to investigate the effect of GPC on the respiratory complexes of the ETS and the coupling of the ATP synthase. Administration of substrates-inhibitors and the uncoupler CCCP was identical to that seen in the IR-linked protocol.

3. The Leak protocol was used to detect the proton leak in mitochondria as follows. In order to determine the leak respiration, liver samples were homogenized in 1 ml of MitOx medium, then 50 μl of homogenates were weighed into the detection chambers. The complex II-linked state II respiration rate was then determined with 10 mM succinate, after the addition of 0.5 μM complex I inhibitor rotenone. To determine the complex II-linked state III respiration, 2.5 mM ADP was added to each chamber. Finally, the leak respiration was measured in the leak state by inhibition of ATP synthase by adding 0.5 μM oligomycin to the medium (state IV respiration).

3.4. Detection of cytochrome c oxidase activity

The cytochrome c oxidase activity was calculated via the time-dependent oxidation of cytochrome c at 550 nm as described previously (Szarka 2004). Briefly, liver samples were homogenized in 10x ice-cold Mitox medium with a Potter grinder, and then centrifuged at 800g for 5 min at 4 °C. Then 50 µl supernatant was added to 2.5 ml cytochrome c stock solution (10.6 mg cytochrome c dissolved in 20 ml distilled water) (Sigma-Aldrich, Budapest, Hungary) and the decrease in optical density at 550 nm was measured spectrophotometrically during 1 min intervals at 0, 30 and 60 min.

3.5. Xanthine oxidoreductase (XOR) activity

Tissue biopsies were homogenized in phosphate buffer (pH 7.4) containing 50 mM Tris.HCl, 0.1 mM EDTA, 0.5 mM dithiotreitol, 1 mM phenylmethylsulfonyl fluoride, 10 µg ml^{-1} soybean trypsin inhibitor and 10 µg ml^{-1} leupeptin. The homogenate was centrifuged at 4 °C for 20 min at 24,000g and the supernatant was loaded into centrifugal concentrator tubes. The activity of XOR was determined in the ultrafiltered supernatant by fluorometric kinetic assay based on the conversion of pterine to isoxanthopterine in the presence (total XOR) or absence (XO activity) of the electron acceptor methylene blue (Beckman 1989).

3.6. NADPH oxidase activity

The NADPH oxidase activity of the liver homogenates was determined by a modified chemiluminometric method of Bencsik *et al.* (Bencsik 2010). The liver samples were homogenized in 2 ml MitOx medium, then 50 µl of resuspended homogenate was added in Dulbecco's solution containing lucigenin (10 mM), EGTA (10 mM) and saccharose (900 mM). The NADPH oxidase activity was determined via the NADPH-dependent increase in luminescence elicited by adding 1 mM NADPH (in 20 µl), measured with an FB12 Single Tube Luminometer (Berthold Detection Systems GmbH, Bad Wildbad, Germany). Samples incubated in the presence of nitroblue tetrazolium served as controls. The measurements were performed in triplicates and were normalized for protein content. The protein content of the samples was determined with Lowry's method.

3.7. Myeloperoxidase (MPO) activity

MPO activity was measured in liver biopsies by the method of Kuebler et al (Kuebler 1996). Briefly, the tissue was homogenized with Tris-HCl buffer (0.1 M, pH 7.4) containing 0.1 M polymethylsulfonyl fluoride to block tissue proteases, and then

centrifuged at 4 °C for 20 min at 24.000 g. The MPO activities of the samples were measured at 450 nm (UV-1601 spectrophotometer; Shimadzu, Japan), and the data were referred to the protein content.

3.8. Whole-blood superoxide and hydrogen peroxide production

10 µl whole-blood and 50 µl zymosan were added to 1 ml Hank's solution (PAA Cell Culture, Westborough, MA, USA) and the mixture was incubated at 37 °C for 30 min, until assay (Ferdinandy 2000). The chemiluminometric response was measured with a Lumat LB9507 luminometer (Berthold Technologies, Wildbad, Germany) during a 30-min period after the addition of 100 µl of lucigenin and luminol reagent.

3.9. MDA assay on liver tissue

The lipid peroxide MDA level was measured through the reaction with thiobarbituric acid, by the method of Placer *et al* (Placer 1966) and corrected for the tissue protein content.

3.10. Liver nitrite/nitrate (NOx) levels

The levels of NOx, the stable end products of NO in the tissues, were measured by the Griess reaction. This assay is based on the enzymatic reduction of nitrate to nitrite, which is then converted into a colored azo compound, which is detected spectrophotometrically at 540 nm (Purnak 2012).

3.11. Reduced glutathione (GSH) and oxidized glutathione disulfide (GSSG) in liver homogenates

The reduced glutathione (GSH) and oxidized glutathione disulfide (GSSG) ratio was determined by using a Fluorimetric Gluthatione Assay Kit (Sigma Aldrich, USA). The GSH content of the sample can be determined by quantifying the thiol concentration in biological samples by reacting with the thiol groups they contain. The adduct can be detected with fluorimetry at 478 nm. The GSSG content of the sample was calculated following the recommendations of the manufacturer.

3.12. Laser-scanning confocal microscopy (CLSEM) and staining protocol

In a separate series fluorescence confocal laser scanning endomicroscopy (CLSEM, Five1, Optiscan Pty. Ltd., Melbourne, Victoria, Australia, excitation wavelength 488 nm; emission detected at 505-585 nm) developed for in vivo histology was employed to detect

the extent of tissue injury in the left liver lobe. The treatments (n=6, each group) were identical to the previous *in vivo* protocol.

The microvascular structure was recorded after the iv administration of fluorescein isothiocyanate-dextran (FITC-dextran, 150 KDa, Sigma-Aldrich, Budapest, Hungary, 10 mg/ml solution dissolved in saline). For the in vivo staining of liver cells, 0.01% acriflavine (Sigma-Aldrich, Budapest, Hungary) was injected into the jugular vein. The objective of the device was placed onto the liver surface, and confocal imaging was performed 5 min after dye administration (1 scan/image, 1024 x 512 pixels and 475 x 475 μm per image).

The analysis was performed twice separately by the same investigator (PH) using a semiquantitative histology score (S0-S4) based on hepatocyte swelling, shrinkage, loss of integrity of cellular and nuclear membranes, or nuclear alterations.

3.13. TUNEL and DAPI staining

Apoptosis was detected by the TUNEL method. For apoptotic cell staining, samples (n=4-6) were analyzed with *In situ* cell death detection kit, TMR red (Roche, Cat. No 12 156 792 910) according to the manufacturer's instructions. Briefly, tissue sections were fixed in 4% paraformaldehyde. For permeabilization, 0.1% Triton X-100 in 0.1% sodium citrate was used. The TUNEL reaction mixture comprised one part Enzyme Solution and nine parts Label Solution. Slides were incubated in a humidified atmosphere for 60 min at 37 °C in the dark, followed by DAPI staining (Sigma-Aldrich®, 1:100). For each experimental series, one negative control (incubated with the Label Solution) and one positive control (digested with DNase I, grade I before application of the TUNEL reaction mixture) samples were used. Three pictures per sample were taken with a Zeiss AxioImager.Z1 microscope at 20x magnification. The number of apoptotic cells per field of view (524.19 μm x 524.19 μm) was determined by Image J 1.47 software.

3.14. Statistical analysis

Data analysis was performed with SigmaStat statistical software (Jandel Corporation, San Rafael, CA, USA). Changes in variables within and between groups were analyzed by two-way repeated measures ANOVA, followed by the Bonferroni test in the cases of the mitochondrial respiratory function, the cytochrome c release from the mitochondria and whole-blood superoxide and H_2O_2 production; one-way ANOVA followed by the Holm-Sidak test was applied in the assay of tissue MDA, XOR activity, MPO activity, NADPH-oxidase activity, tissue nitrite/nitrate, H_2O_2 level and superoxide

level. Data were expressed as means ± SEM. For statistical analysis of TUNEL and DAPI staining, the Kruskal-Wallis and Dunn tests were applied. Histological data were expressed as median ± SD. Values of $P < 0.05$ were considered statistically significant.

4. RESULTS

4.1. IR-induced mitochondrial dysfunctions

The IR-induced changes were investigated with the SUIT protocol. In response to IR injury, both complex I and II basal respiration decreased, as compared with the sham-operated animals, which refer to a lower capacity of the ETS. The ADP-stimulated OxPhos capacity was also decreased at the end of ischemia and throughout the reperfusion phase. Coupling of mitochondrial respiration was significantly damaged in the IR group. Application of selective inhibitors of the mitochondrial complexes (rotenone and antimycin-A) provided evidence for the major role of complex I in IR injury-related mitochondrial dysfunction, as evidenced by decreased oxygen consumption (Figure 4).

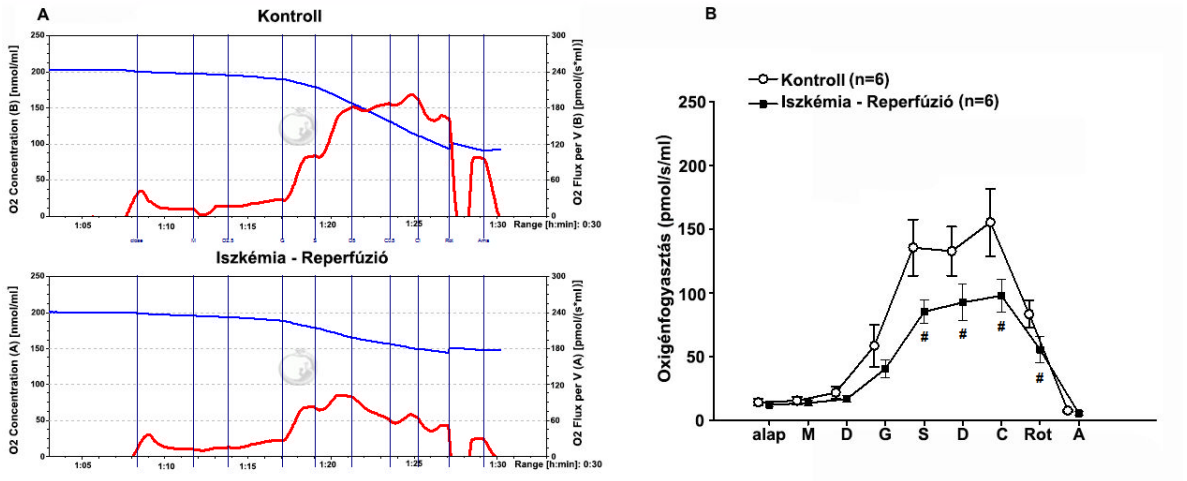

Figure 4. Oxygen consumption of liver homogenates measured by means of high-resolution respirometry (in pmol/s/ml). **A:** Original registration; **B:** SUIT protocol. Animals were subjected to 60 min of liver ischemia followed by 60 min of reperfusion (IR group, black squares) or were sham-operated (SH group, white circles). Data are presented as means ± SEM. $^{\#}P< 0.05$ vs baseline; $^{*}P< 0.05$ vs IR group (two-way ANOVA, Bonferroni test).
bsl: baseline; M: Malate; D: ADP; G: Glutamate; S:Succinate; CCCP: chemical inhibitor of OxPhos (uncoupler); Rot: Rotenone; Ama: Antimycin A.

4.2. Effects of CH_4 on mitochondrial function

Basal mitochondrial respiration in intact mitochondria was determined by adding substrates of complex I (Table 1). The saturating concentration of ADP resulted in a 2-fold increase in complex I-linked respiration, which was not affected by CH_4 treatment. After a stable signal had been reached, complex II-dependent respiration was stimulated by adding succinate which caused a 6-fold increase in both groups. Complex I was then inhibited with rotenone to assess complex II-linked respiration. After complex III inhibition with

antimycin-A, the residual oxygen consumption was equal in the two groups. Finally, ascorbate and TMPD were added to the medium for the measurement of complex IV state III respiration; there was no significant difference in respiratory flux between the groups. Thus, incubation of the respiration medium with 2.2% CH_4 did not affect the activity of OxPhos complexes as compared with room air.

	Glutamate+ Malate	**ADP**	**Succinate**	**Rotenone**	**Antimycin A**	**Ascorbate+ TMPD**
room air	16.4±0.9	34.5±4.5	200.1±15.9	207.1±15.6	9.2±0.6	322.9±37.8
2.2% CH_4	*1.7±1.4*	*36.8±6.0*	*208.1±23.2*	*206.8±21.6*	*6.9±0.5*	*353.6±49.3*

Table 1. Effects of CH_4 incubation on O_2 consumption (pmol/s/ml) of isolated intact liver mitochondria. Data are presented as means ± SEM.

The efficacy of the mitochondrial ETS in response to CH_4 treatment was assessed with a basal protocol from liver homogenates. The complex II-linked respiratory flux values were significantly lower than those of the SH animals at 55 min of ischemia and at 60 min of reperfusion. The IR-induced decreases in basal flux were reversed in response to CH_4 treatment. Interestingly, CH_4 treatment alone (SH+CH_4), elevated the basal oxygen consumption throughout the observation period (Figure 5A).

In comparison with SH, IR resulted in a lower OxPhos capacity of the mitochondria (complex II-linked state III respiration) throughout the examination period. When CH_4 inhalation was applied, however, the respiratory capacity was preserved at 55 min of ischemia and at 30 min of reperfusion (Figure 5B).

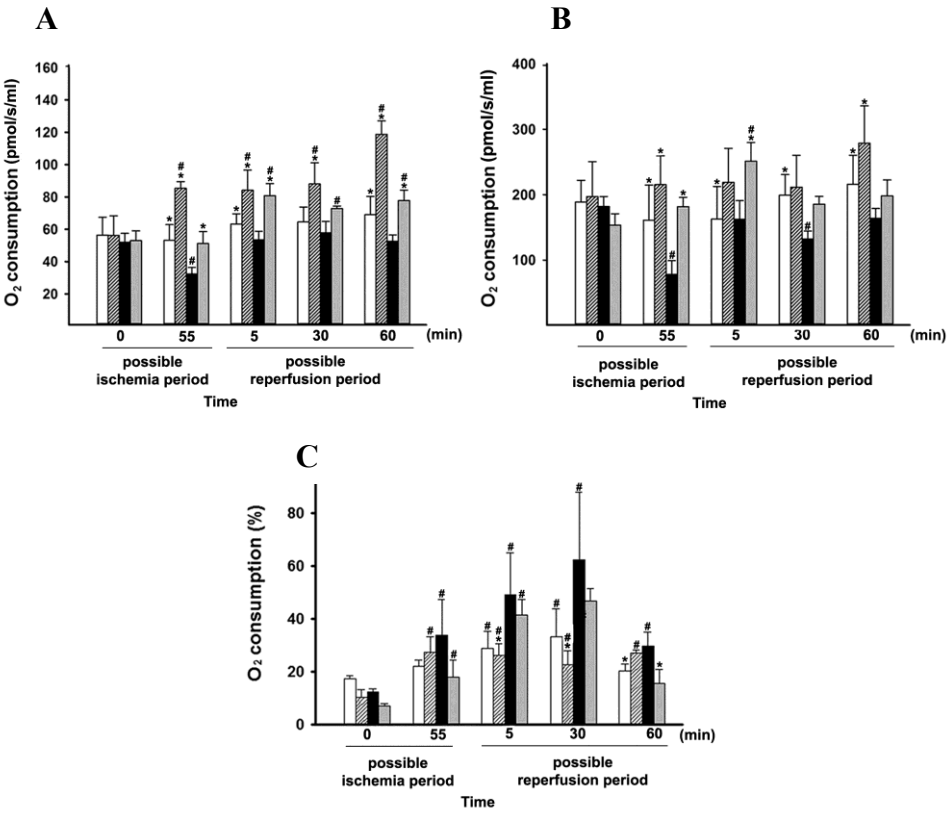

Figure 5. Oxygen consumption of liver homogenates measured by means of high-resolution respirometry. Animals were subjected to 60 min of liver ischemia followed by 60 min of reperfusion (IR group, black column) or were sham-operated (SH group, white column). 2.2% CH_4 inhalation was started 10 min before the end of ischemia and continued throughout the reperfusion (IR+CH_4 group, gray column), or during the identical interval in sham-operated animals (SH+CH_4 group, striped column). **A.** Basal respiration (complex II-coupled state II respiration) (in pmol/s/ml). **B.** Oxidative phosphorylation (complex II-coupled state III respiration) (in pmol/s/ml). **C.** Cytochrome c replacement (state III respiration augmented by adding cytochrome c to the medium) (as % of state III respiration). Data are presented as means ± SEM. $^{\#}$ $P < 0.05$ vs baseline; * $P < 0.05$ vs IR group (two-way ANOVA, Bonferroni test).

4.2.1. Cytochrome c oxidase

The mitochondrial cytochrome c oxidase activity is an indicator of mitochondrial membrane damage (Figure 5C). After IR the ability of exogenous cytochrome c to replace the enzyme in the inner mitochondrial membrane increased significantly, while CH_4 treatment restored the amount of exchanged enzyme to the baseline level. The cytochrome c oxidase activity was also determined with a spectrophotometric analysis (Figure 6). In the SH animals, the cytochrome c level increased minimally as compared with the baseline during the experimental protocol. In the SH+CH_4 group, the enzyme activity decreased in response to CH_4 inhalation. In contrast, the IR group exhibited significantly higher cytochrome c oxidase activities during the reperfusion period, as an indication of functional

damage. In the IR+CH_4 group, the cytochrome c did not increase in response to the IR-induced damage (Figure 6).

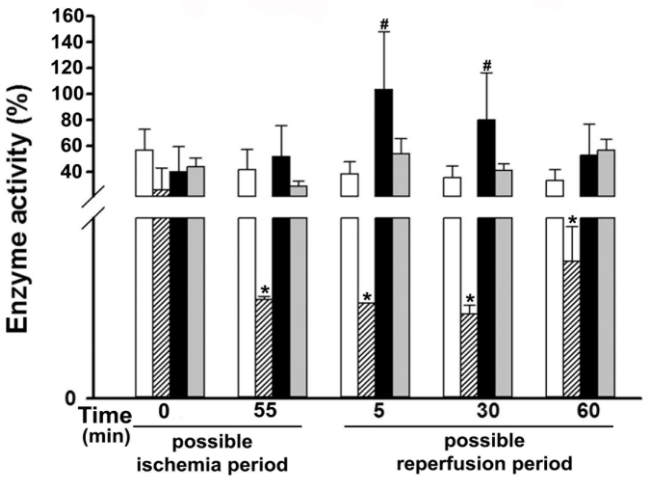

Figure 6. Cytochrome c oxidase activity (in %). Animals were subjected to 60 min of liver ischemia followed by 60 min of reperfusion (IR group, black column) or were sham-operated (SH group, white column). 2.2% CH_4 inhalation was started 10 min before the end of ischemia and continued throughout the reperfusion (IR+CH_4 group, gray column), or during the identical interval in sham-operated animals (SH+CH_4 group, striped column) Data are presented as means ± SEM. $^{\#}P < 0.05$ vs SH group; $^{*}P < 0.05$ vs IR group (two-way ANOVA, Bonferroni test).

4.3. Effects of GPC on mitochondrial function

In vitro experiments were conducted in order to analyse the dose-response effects of GPC on the respiratory activity of rat liver mitochondria in normoxia or anoxic conditions. GPC had an increasing effect on mitochondrial oxygen consumption in the 100-200 mM concentration ranges (Figure 7A). The ETC and OxPhos capacity of mitochondria was influenced significantly when GPC was applied at 200 mM concentration (Figure 7B). In addition, GPC significantly attenuated the deleterious effects of 30-min anoxia on the oxygen consumption of liver mitochondria (Figure 7C).

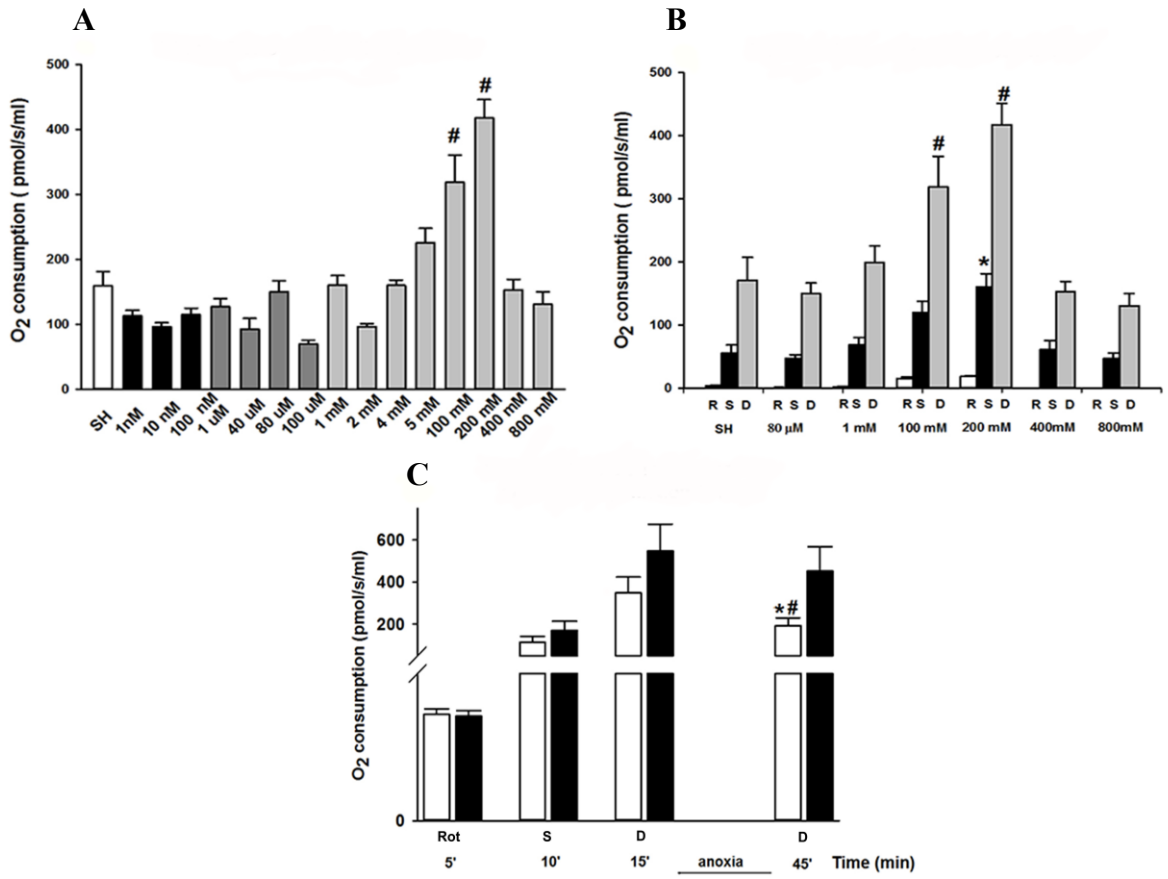

Figure 7. Oxygen consumption (in pmol/s/ml) of liver mitochondria measured by means of high-resolution respirometry. Liver homogenates were harvested from sham-operated animals. **A:** Effect of different GPC concentrations on state III respiration of liver mitochondria. Data are means ± SEM. $^{\#}P< 0.05$ vs SH group (one-way ANOVA, Holm-Sidak test). **B:** Effect of GPC on state II and III respiration. $^{\#}P< 0.05$ vs SH (state II) group; $^{*}P< 0.05$ vs SH (state III) group (one-way ANOVA, Holm-Sidak test). **C:** Effect of 200 mM GPC on mitochondrial anoxia-reoxygenation *in vitro*. Liver homogenates were subjected to 30' anoxia in the presence of 200 mM GPC (black column: SH+GPC group) or without GPC pre-treatment (white column: SH group). Data are presented as means ± SEM. $^{\#}P< 0.05$ vs 5'; $^{*}P< 0.05$ vs SH group (two-way ANOVA, Bonferroni test).
R: Rotenone; S: Succinate; D: ADP

The effects of GPC on IR-induced mitochondrial dysfunction were evaluated with the SUIT protocol (Figure 8A). The state III oxygen consumption was significantly lower in IR compared to the sham-operated animals. Additionally, the maximum respiratory capacity was also significantly lower in response to the IR stress. In contrast, treatment with GPC enhanced the efficacy of oxygen consumption. These effects were basically linked to the complex I, rather than complex II, as indicated by the large decrease following the administration of the inhibitor of complex I.

The Leak protocol (Figure 8B) demonstrated significant decrease in state IV oxygen consumption in response to IR injury as compared to the sham-operated animals. GPC

administration restored the level of leak respiration to that of the sham-operated animals.

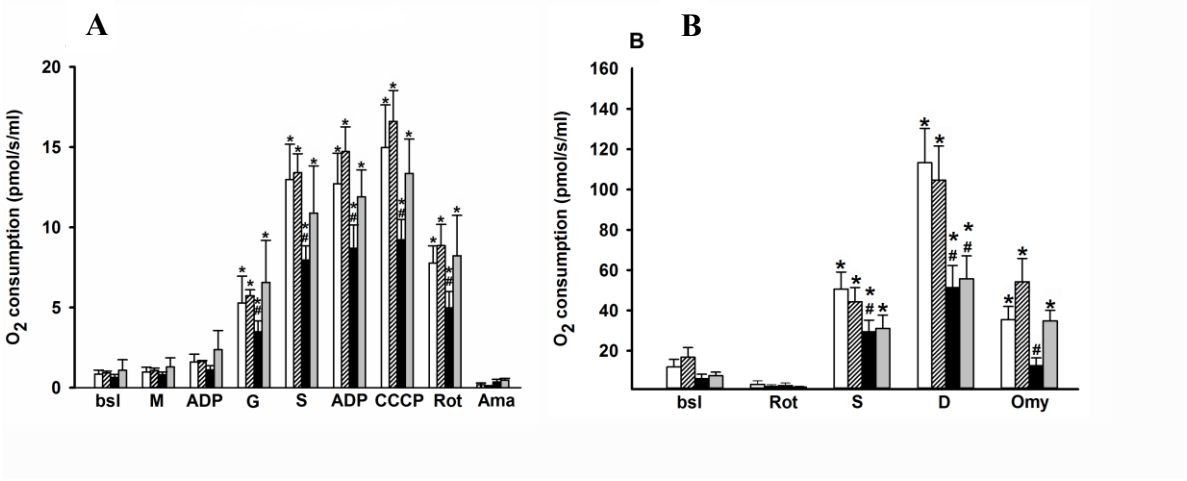

Figure 8. Oxygen consumption of liver mitochondria measured by means of high-resolution respirometry (in pmol/s/ml). **A:** SUIT protocol. **B:** Leak protocol. Animals were subjected to 60 min of liver ischemia followed by 60 min of reperfusion (IR group, black column) or were sham-operated (SH group, white column). 16.56 mg/kg GPC administration was started 5 min before the end of ischemia (IR+GPC group, grey column), or at identical time point in sham-operated animals (SH+GPC group, white striated column). Data are presented as means ± SEM. #P< 0.05 vs SH group; *P< 0.05 vs baseline (two-way ANOVA, Bonferroni test).
bsl: baseline; M: Malate; D: ADP; G: Glutamate; S:Succinate; CCCP: chemical inhibitor of OxPhos (uncoupler); Rot: Rotenone; Ama: Antimycin A; Omy: Olygomycin

4.4. Effects of CH_4 on oxidative damage and structural changes

4.4.1. Blood superoxide and H_2O_2 production

The whole-blood superoxide-producing capacity was significantly higher in the IR group at 30 min of reperfusion in comparison with the SH animals. The CH_4 inhalation before the end of the ischemic period reduced the elevated superoxide production to the level in the SH animals (Figure 9A). Significantly higher whole-blood H_2O_2 levels were measured at 5, 30 and 60 min of reperfusion in the IR group relative to the SH group. The CH_4 inhalation protocol effectively reversed H_2O_2 production in the IR+ CH_4 group (Figure 9B).

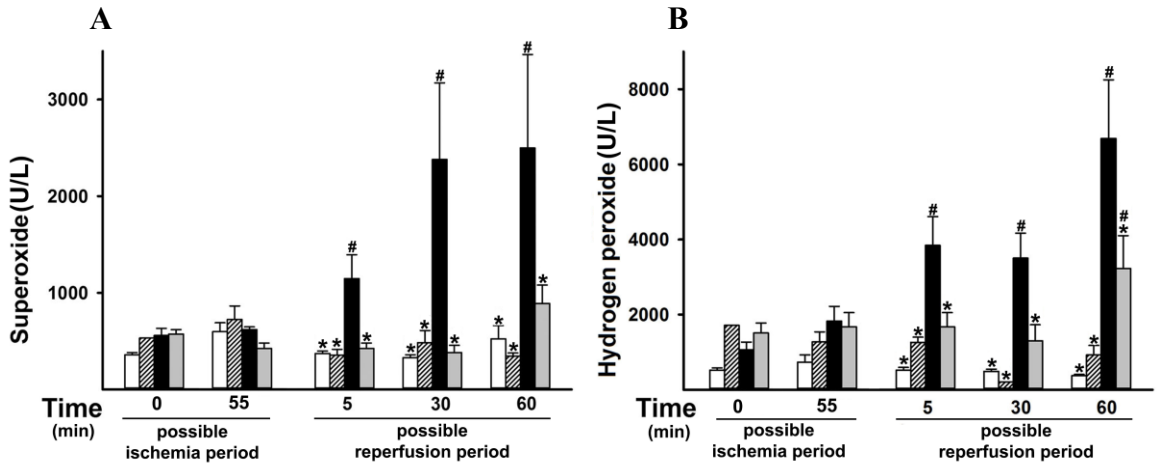

Figure 9. Superoxide and H_2O_2 production in the whole-blood. Animals were subjected to 60 min of liver ischemia followed by 60 min of reperfusion (IR group, black column) or were sham-operated (SH group, white column). 2.2% CH_4 inhalation was started 10 min before the end of ischemia and continued throughout the reperfusion (IR+CH_4 group, gray column), or during the identical interval in sham-operated animals (SH+CH_4 group, striped column) **A.** Superoxide level (in U/L), **B.** H_2O_2 level (in U/L). Data are presented as means ± SEM. $^{\#}$ $P < 0.05$ vs SH group; * $P < 0.05$ vs IR group (two-way ANOVA, Bonferroni test).

4.4.2. Tissue MDA level

A significantly higher MDA level was measured at the end of reperfusion in the IR group than in the SH group. The IR-induced elevation of the liver MDA level was effectively attenuated by CH_4 inhalation in the IR+CH_4 group (Figure 10).

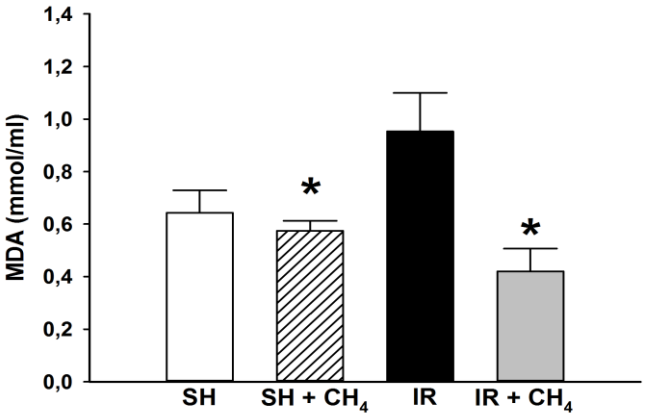

Figure 10. Tissue MDA level (in mmol/ml). **A:** Animals were subjected to 60 min of liver ischemia followed by 60 min of reperfusion (IR group, black column) or were sham-operated (SH group, white column). 2.2% CH_4 inhalation was started 10 min before the end of ischemia and continued throughout the reperfusion (IR+CH_4 group, gray column), or during the identical interval in sham-operated animals (SH+CH_4 group, striped column). Data are presented as means ± SEM. $^{\#}$ $P < 0.05$ vs SH group; $^{*}P < 0.05$ vs IR group (one-way ANOVA, Holm-Sidak test).

4.4.3. *In vivo* morphological changes

The morphological changes in the left liver lobe were evaluated by means of *in vivo* imaging, using confocal laser scanning endomicroscopy. The FITC-dextran and acriflavine staining demonstrated more dilated sinusoids in the IR group, and also histological signs of apoptosis: a loss of fluorescence intensity, changes in hexagonal cell shape and cytoplasm blebbing and vesicle formation relative to the SH group. CH_4 inhalation effectively attenuated these apoptosis-linked morphological changes (Figure 11).

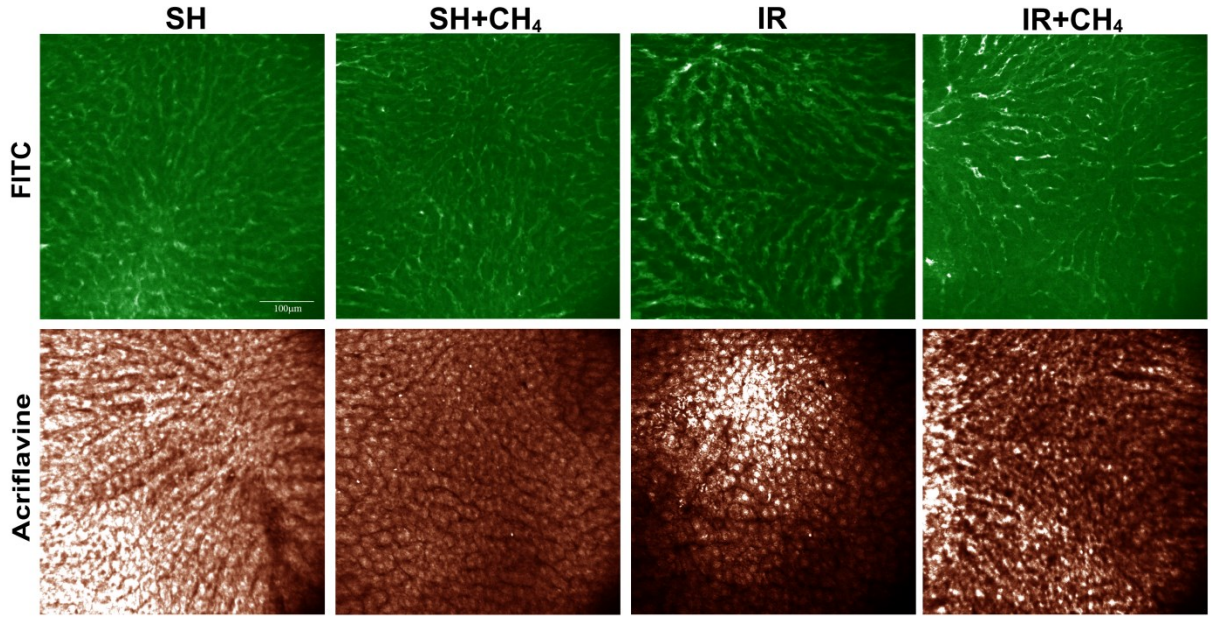

Figure 11. Histological changes in the rat liver. Tissue sections show the results of *in vivo* confocal laser scanning endomicroscopy with FITC dextran and acriflavine labeling. Apoptosis-related structural changes such as dilated sinusoids, loss of fluorescence intensity, changes in hexagonal cell shape, cytoplasmatic blebbing and vesicle formation can be observed in the IR group. The bar represents 100 µm.

4.4.4. Apoptosis

As expected, few TUNEL-positive cells were observed in the liver specimens of the rats in the SH+CH_4 and SH groups. Conversely, liver IR was accompanied by an increased TUNEL positivity, which was diminished as a result of CH_4 inhalation (IR and IR+CH_4 groups) (Figure 12).

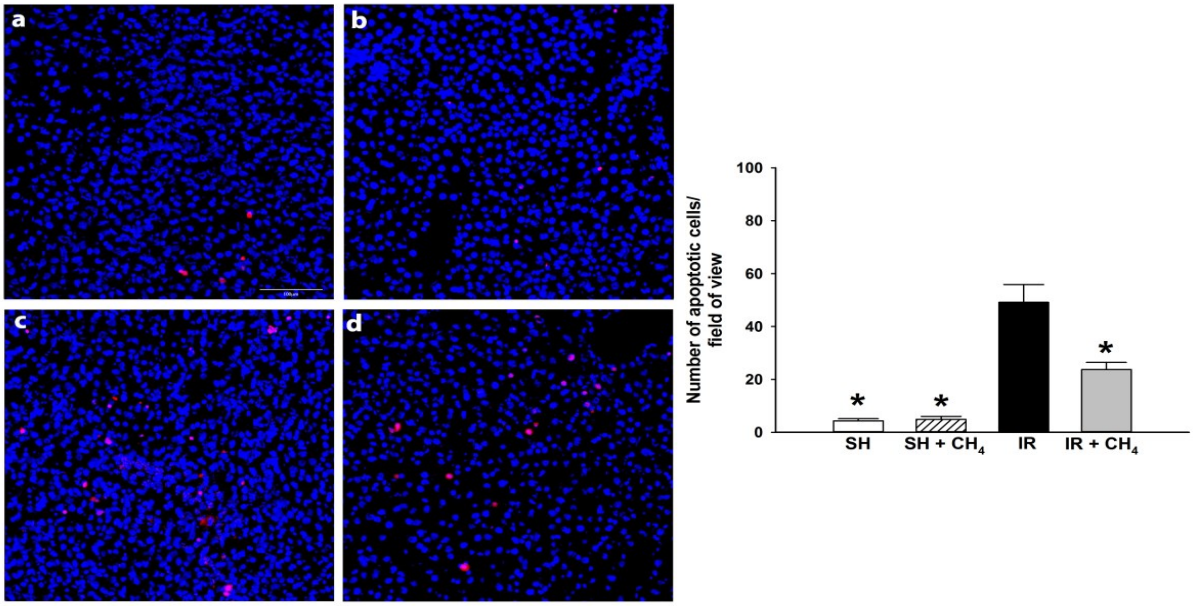

Figure 12. Liver cell apoptosis. Tissue sections are labeled with TUNEL/DAPI staining. **a.** SH group, **b.** SH+CH_4 group, **c.** IR group, **d.** IR+CH_4 group. Nuclei are marked in blue, and apoptotic nuclei in red. Data are presented as median ± SD. * $P < 0.05$ vs IR group (Kruskal-Wallis and Dunn tests).

4.5. Effects of GPC on oxidative damage

4.5.1. XOR activity

XOR is a key enzyme in purine catabolism, and also catalyses the reduction of nitrates and nitrites into nitric oxide (NO). During this process, ROS are produced, which can be deleterious to the cells. As expected, XOR activity was increased in the IR group compared to the SH group. These values were significantly decreased when GPC was applied 5 min before the reperfusion (Figure 13).

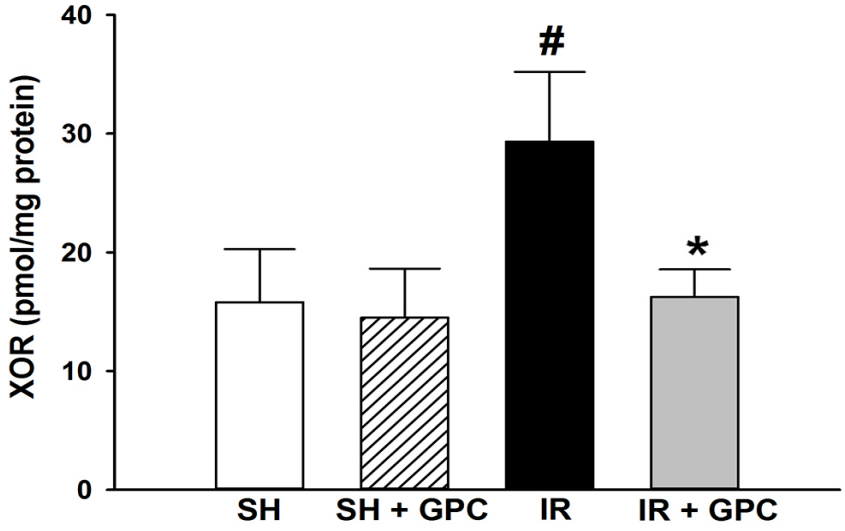

Figure 13. XOR activity (in pmol/mg protein). Animals were subjected to 60 min of liver ischemia followed by 60 min of reperfusion (IR group, black column) or were sham-operated (SH group, white column). 16.56 mg/kg GPC administration was started 5 min before the end of ischemia (IR+GPC group, grey column), or at identical time point in sham-operated animals (SH+GPC group, white striated column). Data are presented as means ± SEM. $^{\#}P< 0.05$ vs SH group; *P< 0.05 vs IR group (one-way ANOVA, Holm-Sidak test).

4.5.2. NADPH oxidase activity

NADPH oxidases are a family of membrane-bound oxidoreductase complexes whose main function is the formation of ROS, by catalysing the reduction of oxygen ($2NADPH + 2O_2 \rightarrow 2NADP^+ + 2H^+ + 2O_2^- \rightarrow 2NADP^+ + H_2O_2$). While their precise role in the IR pathogenesis is not fully elucidated, it is assumed that NADPH oxidases play a key role in the propagation of oxidative stress. By the end of the 60-min reperfusion period, the NADPH oxidase activity was significantly increased in the IR group, compared to the SH groups (Figure 14). When GPC was administered before the end of ischemia the NADPH oxidase activity became even lower than the values of the SH groups.

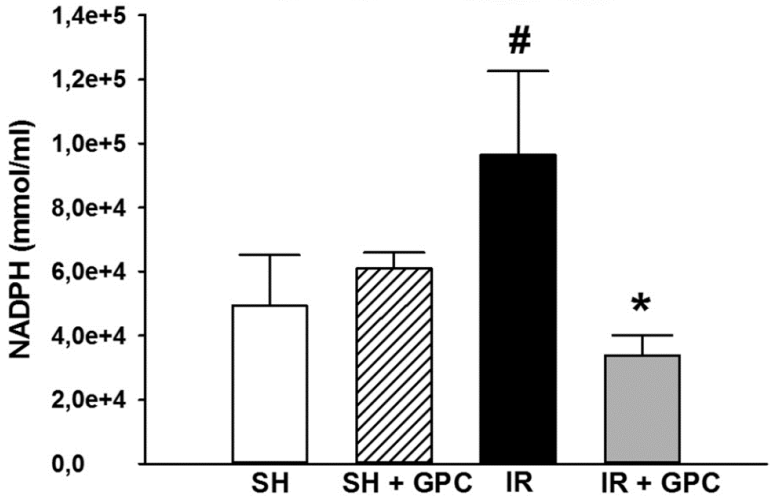

Figure 14. NADPH oxidase activity (in mmol/ml). Animals were subjected to 60 min of liver ischemia followed by 60 min of reperfusion (IR group, black column) or were sham-operated (SH group, white column). 50 mg/kg GPC administration was started 5 min before the end of ischemia (IR+GPC group, grey column), or at identical time point in sham-operated animals (SH+GPC group, white striated column). Data are presented as means ± SEM. $^{\#}P< 0.05$ vs SH group; $^{*}P< 0.05$ vs IR group (one-way ANOVA, Holm-Sidak test).

4.5.3. MPO activity

MPO is mostly produced by PMN leukocytes upon their activation. In the vehicle-treated IR group, the tissue MPO level was significantly increased as compared with that of the sham-operated animals. In the GPC-treated group, the MPO activity was significantly

lower than in the vehicle-treated IR group (Figure 15).

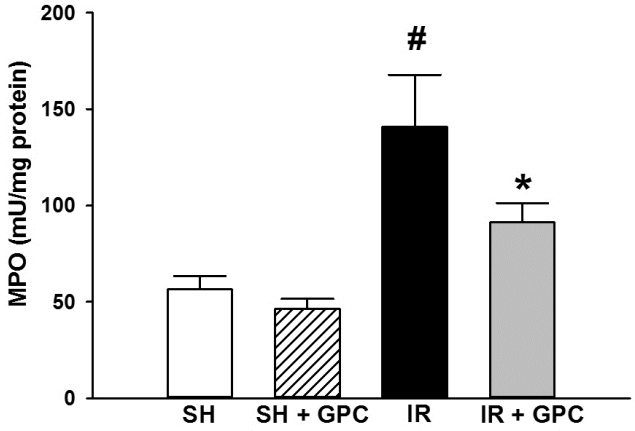

Figure 15. Tissue MPO activity (in mU/mg protein). Animals were subjected to 60 min of liver ischemia followed by 60 min of reperfusion (IR group, black column) or were sham-operated (SH group, white column). 16.56 mg/kg GPC administration was started 5 min before the end of ischemia (IR+GPC group, grey column), or at identical time point in sham-operated animals (SH+GPC group, white striated column). Data are presented as means ± SEM. $^{\#}$ *P*< 0.05 vs SH group *P< 0.05 vs IR group (one-way ANOVA, Holm-Sidak test).

4.5.4. Blood superoxide and H_2O_2 production

The superoxide-producing capacity in the whole blood was significantly higher in the IR group at the end of reperfusion when compared to the SH animals. The GPC treatment before the end of the ischemic period reduced the elevated superoxide production to the level in the control animals (Figure 16A). Significantly higher whole blood H_2O_2 levels were measured at the end of reperfusion in the IR group relative to the SH group, and the GPC treatment effectively reversed the H_2O_2 production (Figure 16B).

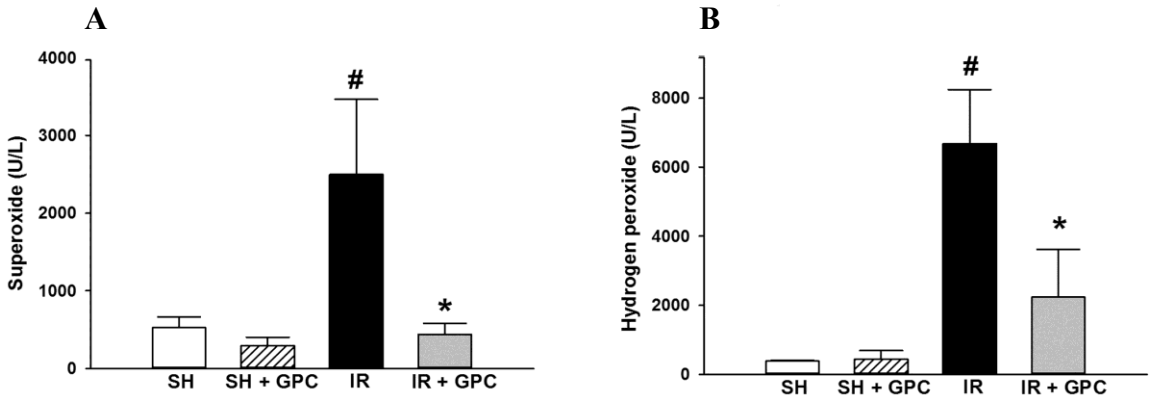

Figure 16. Superoxide and H_2O_2 production in the whole-blood. Animals were subjected to 60 min of liver ischemia followed by 60 min of reperfusion (IR group, black column) or were sham-operated (SH group, white column). 16.56 mg/kg GPC administration was

started 5 min before the end of ischemia (IR+GPC group, grey column), or at identical time point in sham-operated animals (SH+GPC group, white striated column). **A:** Superoxide level (in U/L); **B:** H_2O_2 level (in U/L). Data are presented as means ± SEM. $^{\#}P< 0.05$ vs SH group; $^{*}P< 0.05$ vs IR group (one-way ANOVA, Holm-Sidak test).

4.5.5. Tissue MDA level

As expected, IR resulted in an increased MDA production after IR (Figure 17). The GPC treatment reduced the level of MDA production, while no difference was seen between the two control groups (SH and SH+GPC).

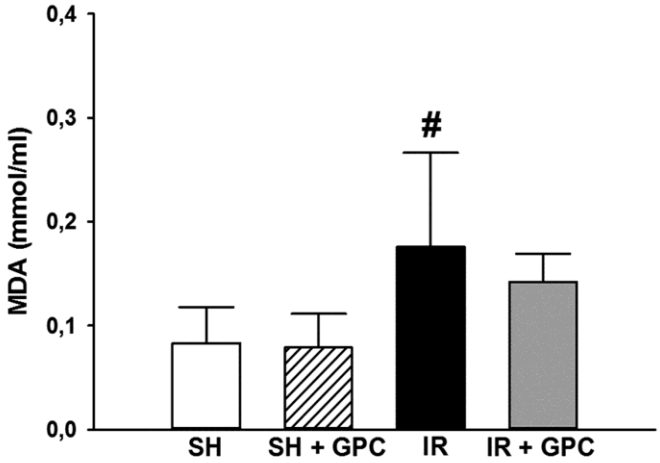

Figure 17. Tissue MDA level (in mmol/ml). Animals were subjected to 60 min of liver ischemia followed by 60 min of reperfusion (IR group, black column) or were sham-operated (SH group, white column). 16.56 mg/kg GPC administration was started 5 min before the end of ischemia (IR+GPC group, grey column), or at identical time point in sham-operated animals (SH+GPC group, white striated column). Data are presented as means ± SE. $^{\#}P< 0.05$ *vs* SH group; (one-way ANOVA, Holm-Sidak test).

4.5.6. Liver NOx levels

In the IR group, a significant elevation in NOx was present relative to the SH groups. The GPC treatment protocol decreased the NOx elevation, in contrast with the non-treated IR group; but the NOx level remained higher than that in the sham-operated group (Figure 18).

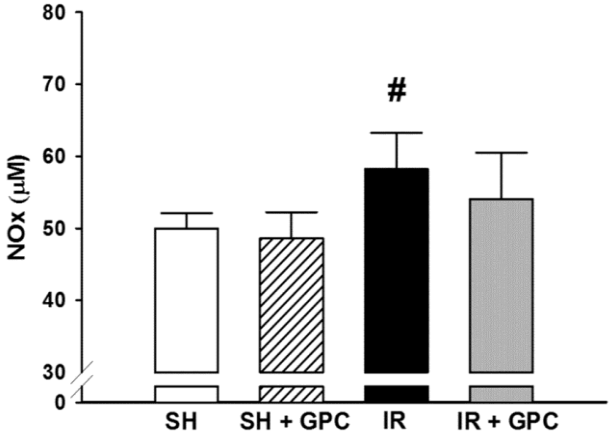

Figure 18. Tissue nitrite/nitrate (NOx) level (in μM). Animals were subjected to 60 min of liver ischemia followed by 60 min of reperfusion (IR group, black column) or were sham-operated (SH group, white column). 16.56 mg/kg GPC administration was started 5 min before the end of ischemia (IR+GPC group, grey column), or at identical time point in sham-operated animals (SH+GPC group, white striated column). Data are presented as means ± SEM. $^{\#}P< 0.05$ vs SH group; (one-way ANOVA, Holm-Sidak test).

4.5.7. GSH/GSSG ratio in liver homogenates

GPC administration in the SH+GPC group did not influence the GSH/GSSG ratio as compared with the SH group. As expected, hepatocytes were exposed to increased levels of oxidative stress after IR, as shown by a significant increase of GSSG and the decreased GSH/GSSG ratio when compared to the SH group, however, the GSSG levels were significantly decreased in response to GPC treatment in the IR+GPC group (Figure 19).

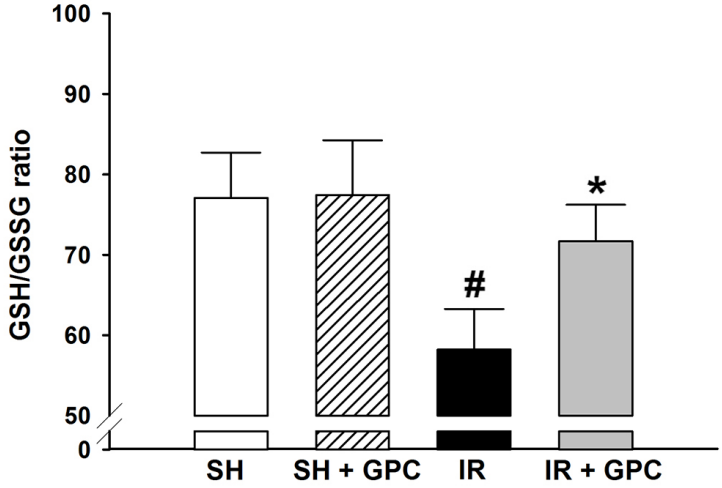

Figure 19. GSH/GSSG ratio. Animals were subjected to 60 min of liver ischemia followed by 60 min of reperfusion (IR group, black column) or were sham-operated (SH group, white column). 16.56 mg/kg GPC administration was started 5 min before the end of ischemia (IR+GPC group, grey column), or at identical time point in sham-operated animals

(SH+GPC group, white striated column). Data are presented as means ± SEM. # P< 0.05 vs SH group *P< 0.05 vs IR group (one-way ANOVA, Holm-Sidak test).

4.5.8. *In vivo* histology

The morphological changes in the left liver lobe were evaluated by means of *in vivo* imaging, using confocal laser scanning endomicroscopy. The FITC-dextran and acriflavine staining demonstrated dilated sinusoids in the IR group, fluorescent dye leakage with edema formation was present with visible signs of structural damage: changes in hexagonal cell shape and cytoplasm blebbing and vesicle formation. GPC administration effectively attenuated the IR-induced morphological changes. The severity of injury was moderated, these changes were still apparent, but the average degree of damage was decreased from S4 to S2 level (Figure 20).

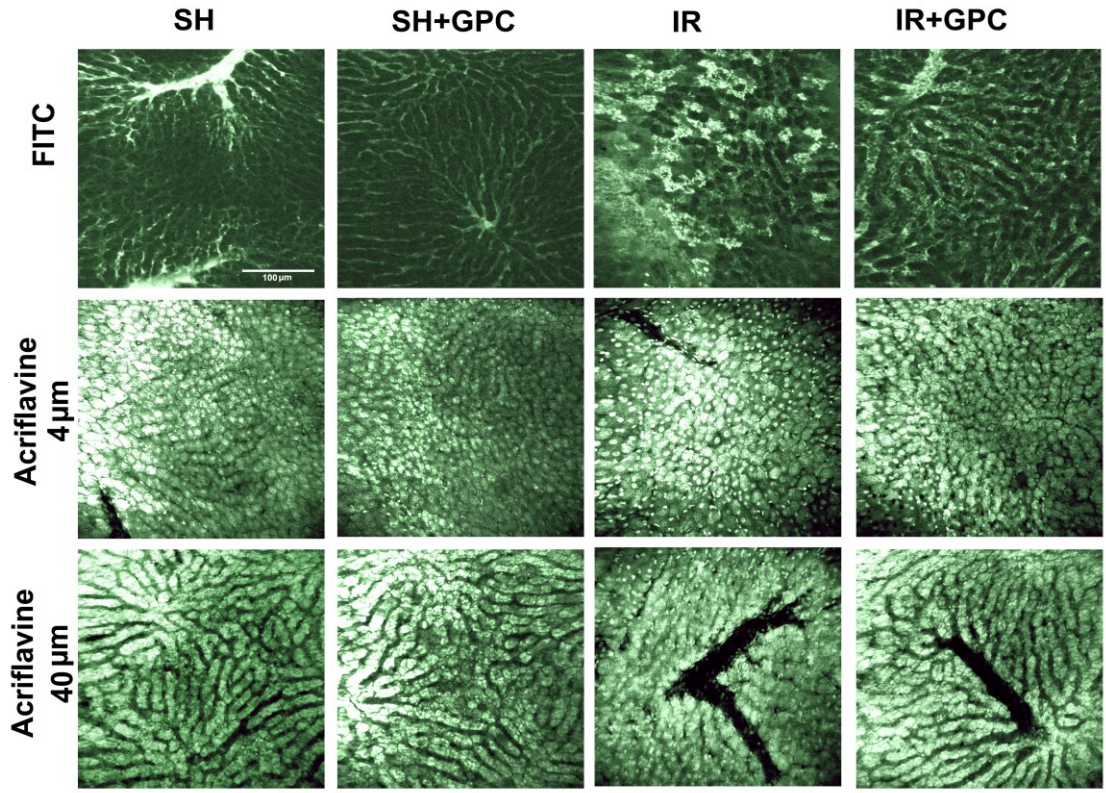

Figure 20. Histological changes in the rat liver. Tissue sections show the results of *in vivo* fluorescence confocal laser scanning endomicroscopy with FITC dextran and acriflavine labelling (at 4 and 40 µm depth). Structural damages such as dilated sinusoids, loss of fluorescence intensity, changes in hexagonal cell shape, cytoplasmatic blebbing and vesicle formation can be observed in the IR group. The bar represents 100 µm.

5. DISCUSSION

5.1. IR-induced changes in mitochondrial functions

Low-flow states, trauma, liver resection surgery for treatment of benign and malignant disease, and liver transplantation are some of the scenarios that predispose the liver to IR (Lei 2001; Kiemer 2002). With the lack of the final electron acceptor, oxygen, the electron flow in the respiratory chain is immediately interrupted, leading to a reduced activity of ATP synthase. Meanwhile, mitochondria no longer accept electrons from substrates; therefore, the number of pyridine nucleotides are reduced, resulting in an increased intracellular NADH/NAD^+ ratio.

Our experiments revealed the non-phosphorylating basal respiration of complex II in the presence of the reducing succinate substrate, but in the absence of ADP. State II respiration is the resting state of intrinsic uncoupled or dyscoupled respiration, when the oxygen flux is maintained in order to compensate for the proton leak at a high chemiosmotic potential when ATP synthase is not active. ADP-dependent oxygen consumption is a test of mitochondrial functional integrity and its overall function which directly reflects mitochondrial OxPhos (Li 2012). The ADP-stimulated respiration of coupled mitochondria (OxPhos or state III) was supported by high, saturating concentrations of ADP and was significantly increased, by ~ 60%, in the sham-operated animals.

In response to IR-injury, the basal respiratory activity of mitochondria significantly decreased, which refers to a lower capacity of the respiratory chain to transmit electrons toward the ATP synthase. The ADP-stimulated OxPhos capacity also decreased at the end of ischemia and throughout the reperfusion phase. The application of selective substrates and inhibitors of the mitochondrial complexes provided evidence for the major role of complex I in IR injury, as demonstrated by decreased oxygen consumption and the increased leak respiration.

In the leak state of mitochondria, oxygen flux is maintained mainly to compensate for the proton leak at a high chemiosmotic potential through the respiratory complexes, when the ATP synthase is not active. Leak respiration is measured in the presence of reducing substrate, but in the absence of ADP. Dyscoupling of mitochondria in IR led to an increased superoxide formation and membrane damage. Peroxidation, an immediate chain reaction, caused the breakdown of biomembranes, leading to decompartmentalization and to

the loss of maintenance of a steady state.

As a consequence of mitochondrial distress, the intracellular redox milieu changes, and this leads to an alteration in intracellular enzyme activity. Accordingly, mitochondria-derived superoxide formation contributes to intracellular ROS formation through different ways (1) by being the primary source of production and (2) as a modifier of other intracellular superoxide producing enzymes activity, too. In our studies, we examined the activities of the main extra-mitochondrial enzymatic complexes responsible for ROS formation, XOR and NADPH oxidase. The IR-induced increases in superoxide and H_2O_2 levels in the circulating blood were accompanied by increased local NOx concentrations, providing indirect evidence for an evolving nitroxidative stress in the liver tissue.

5.2. Effects of CH_4 in mitochondrial dysfunction

Normoxic ventilation with 2.5% CH_4 supplementation has been shown to protect the intestinal tissues and mitigate liver injury after an IR insult (Boros 2012). Recently, fundamental evidence has accumulated to demonstrate the anti-inflammatory and antiapoptotic properties of CH_4-based treatments in various IR settings; however, its intracellular target has remained elusive (Song 2015, Wu 2015, Ye 2015, Chen 2016, He 2016). Mitochondria are critically involved in hypoxia-reoxygenation-induced intracellular respiratory damage; therefore, they are possible targets of CH_4 administration.

In our study, we investigated the *in vivo* influence of an increased CH_4 intake on the respiratory activity of rat liver mitochondria by using controlled ventilation. This protocol did not influence the blood-gas chemistry in the anesthetized animals under the baseline conditions. More importantly, the inhalation of CH_4-containing normoxic artificial air preserved the OxPhos after a period of tissue ischemia, and significantly improved the basal mitochondrial respiration state after the onset of reperfusion. In line with this, IR-induced ROS production, cytochrome c release and hepatocyte apoptosis were also significantly reduced.

It is known that ~ 2-4% of the electrons flowing through the ETC generate superoxide anions by the partial reduction of oxygen (Lesnefsky 2001; Tahara 2009), i.e. involving precursors of ROS such as H_2O_2 and OH^-, and our data provide evidence for the influence of an increased CH_4 intake on mitochondrial ETC reactions. However, the exact pathway through which CH_4 influences the mitochondrial respiration has remained unexplored, and several mechanisms can be postulated to explain the *in vivo* effects of CH_4 in this system.

In this respect, data overall support a role for CH_4 membrane defense during ROS-induced damage. During ischemia, the mitochondrial NADH/NAD^+ and FADH/FAD^+ ratios remain elevated, leading to reductive stress (Ghyczy 2008; Boros 1999), while reperfusion of the previously ischemic tissue leads to oxidative stress with a burst of ROS generation following the start of reoxygenation. It was earlier suggested (without indicating the exact biochemistry, contributing compounds or enzymes) that ROS reactions could lead to a higher level of fixation of CH_4 in a lipid environment, such as the mitochondrium membrane (Carlisle 2005; Dougherty 1967). Indeed, IR perturbs the heterogeneous lipid-bilayer membrane structure and changes the fluidity from fluid to gel. Disordered/fluidized bilayer states could therefore be analogous to physical damage to the ETC in these conditions. Inhaled exogenous CH_4 will move from the alveoli into the circulation, and diffuse into the plasma, throughout which it is rapidly and evenly distributed. If there are no barriers, the apolar CH_4 may enter the cytoplasm and mitochondrial matrix and dissolve in the hydrophobic nonpolar lipid tails of the phospholipid biomembranes (Meyer 1980). Membrane rigidity relates to the degree of lipid peroxidation, when the level of oxidized lipids is increased and the fluidity of membranes is reduced. CH_4 dissolved in biological membranes may affect this process, thereby influencing the stereo structure of membrane proteins, which determines their accessibility and morphology (Levine 1996). The peroxidation of polyunsaturated fatty acids and a direct triggering of cytochrome c release from the mitochondria are well-known consequences of IR injury (McCord 1985). The degree of lipid peroxidation can be estimated via the amount of MDA, a marker of oxidative damage of lipid membranes. As a reactive aldehyde, MDA is one of the many reactive electrophilic compounds that cause further oxidative stress in cells and form covalent protein adducts referred to as advanced lipoxidation end-products. We have shown that the levels of both ROS and MDA were reduced after an increased CH_4 intake, indirectly demonstrating the decreased oxidative damage to the mitochondrial membranes.

Furthermore, CH_4 may accumulate transiently at cell membrane interfaces, thereby transitorily changing the physico-chemical properties or the *in situ* functionality of proteins, ion channels and receptors embedded within this environment. In this case, an increased CH_4 intake may influence the function of membrane-bound structures. The pilot *in vitro* results demonstrated that the incubation of isolated mitochondria in a 2.2% CH_4 atmosphere has no effect on the respiratory activity of the ETC. As opposed to this, the *in vivo* CH_4 inhalation regimen unexpectedly increased the mitochondrial respiratory function, without

influencing the baseline ROS production in the SH animals. These differing responses can also be explained by membrane injury, as compared to isolated mitochondria, homogenation can disrupt mitochondrial membranes (Picard 2011). In contrast, the protocol of mitochondria isolation permits rearrangement of the membranes and results in fully viable mitochondria whose function cannot be further ameliorated by CH_4 (Gnaiger 2000).

This study addressed the plausibility of CH_4 bioactivity. This concept is supported by experimental data showing that gaseous CH_4 can delay the contraction of peristalsis and increase the amplitude of the peristaltic contractions in the guinea pig ileum (Pimentel 2006). A recent study provided *in vitro* evidence that CH_4 can inhibit the contractile activity of the smooth muscle by activating the voltage-dependent potassium channels and increasing the voltage-dependent potassium current (Liu 2013).

Whereas the results indicate a bioactive role for higher concentrations of exogenous CH_4, this is not obvious for endogenous sources. It is widely recognized that large amounts of CH_4 can be produced by the anaerobic metabolism of methanogenic microorganisms in the GI tract (Attaluri 2010; Roccarina 2010), and CH_4 is present in measurable amounts in the breath of approximately one-third of humans (Levitt 2006). Nevertheless, as opposed to the previous view, *in vitro* and *in vivo* studies have revealed the possibility of nonmicrobial CH_4 formation in both plants and animals (Keppler 2009; Tuboly 2013). CH_4 generation has been demonstrated after site-specific inhibition of the ETC, and in association with a mitochondrial dysfunction, similarly to the effects of hypoxia (Ghyczy 2008; Tuboly 2013). Of interest, recent studies demonstrated the critical role of a ferryl species ($[Fe(IV)=O]^{2+}$) and CH_3 radicals, leading to the *in vitro* generation of CH_4 from methionine sulfoxide as substrate at ambient temperature (Althoff 2010). In this chemical reaction, CH_4 is readily formed from the S-CH_3 groups of organosulfur compounds in a model system containing iron(II/III), H_2O_2 and ascorbate that uses organic compounds with heterobonded CH_3 groups for CH_4 generation under ambient (1,000 mbar and 22^oC) and aerobic (21% oxygen) conditions. CH_3 radicals can be formed in the mitochondria through reaction between a reducing agent, a metal and a hydroperoxide. Methionine is known to be a key factor in many biochemical reactions in plants, fungi and animals, and methionine residues in the surface of proteins are highly susceptible to oxidation, the product generally being methionine sulfoxide. Importantly, the available data suggest that reversible methionine oxidation could be a novel mechanism in redox - regulation, which involves the repair mechanism of methionine sulfoxide reductases (MSRs) whose main function is to protect

membranes from oxidative damage (Levine 1996). The MSRs were originally thought to be exclusively bacterial enzymes, but their presence was recently proven in mitochondria in mammals (Weissbach 2005). The scavenging action of these enzymes is based on the cyclic oxidation and reduction of the several methionine residues of the molecules that makes them the counterpart of the NADH/NAD^+ system (Levine 1996). In an oxygen-depleted environment, the methionine sulfoxide-CH_4 system may act as an alternative to NADH/NAD^+ and FADH/FAD^+ as an electron donor, thereby mitigating ischemia-induced reductive stress. The capacity of mitochondria to reverse oxidant-induced changes upon reperfusion originates from the exposure of previously hidden epitopes of mitochondrial proteins, as proven in the case of mitochondrial MSRs (Cole 2010).

IR injury is an antigen-independent stimulus that initiates intrinsic signaling pathways. Cytochrome c is attached to the inner membrane, and is detached in response to a threshold disturbance in the membrane structure, which leads to activation of the apoptotic caspase cascade (Wang 2001). CH_4 inhalation effectively attenuated the IR-induced elevation in MDA level, and in parallel, the amount of cytochrome release was diminished. Conventional and *in vivo* histology provided evidence of IR-related apoptosis and the observations suggest that CH_4 may influence the cell fate under stress conditions.

5.3. Effects of GPC in ROS production

GPC is a well-known protective compound in IR-injuries; however, the exact mechanism of action has not been described. In our studies, we have outlined a novel route of action for the molecule. The *in vitro* experimental data demonstrated the direct effects of GPC on mitochondrial oxygen consumption in the 100 and 200 mM concentration ranges. Next, GPC supplementation attenuated the respiratory consequences of anoxia by reducing the leak of protons into the matrix. This effect had mainly been attributed to an action on complex I at the appropriate concentration of 200 mM. Within the mitochondria, the mechanism by which GPC increases basal oxygen consumption rates is not well-understood, nevertheless, there are two plausible explanations: 1) by interacting with proteins and causing modulations in their functions or 2) by influencing the redox environment. Furthermore, the I-V sequence of the respiratory complexes is perhaps not the highest level of OxPhos organization. Flux control experiments confirm that the respiratory chain operates as one single functional unit (Bianchi 2004; Boumans 1998). According to the “fluid-state model”, individual protein complexes of the electron transport chain freely diffuse in the membrane and the electron transfer is based on random collisions of single

complexes. Recent findings also suggest that OxPhos enzymes are organized into supramolecular assemblies (Lenaz 2009). It has been shown that point mutations in genes of the subunits of an OxPhos complex affect the stability of another complex. Thus, complex III and complex IV are necessary for the assembly or stability of complex I (Acín-Pérez 2004; Diaz 2006). Moreover, it appears that supercomplexes are further organized into larger string structures. The example is the ATP synthase complex (complex V), which assembles into long oligomeric chains (Krause 2005). Some supercomplexes require an appropriate osmotic environment for their formation (Zhang 2002; Pfeiffer 2003). Whether GPC influences the conformation of this system is an open question.

Secondly, the redox-optimized ROS balance hypothesis postulates that the redox environment is the main controller of both production and scavenging of ROS as an intermediary between mitochondrial respiration and ROS formation (Aon 2010). We have shown that exogenous GPC targets the mitochondrial oxidative metabolism in IR stress, and have provided evidence that this way the IR-associated inflammatory activation may be limited. Mitochondrial dysfunction generates ROS and hypoxic conditions induce a leak of electrons of the ETC into the intermembranous space (Rose 2014), which can lead to increased ROS formation. We have demonstrated that GPC treatment reduces the leak respiration after an IR challenge, and in accordance with previous findings, the lower leak respiration was accompanied with a decreased ROS formation (Scribner 2010; Rose 2014; Kenneth 2005). Furthermore, exogenous GPC enhanced mitochondrial oxygen consumption both in normoxic and hypoxic conditions, which clearly demonstrates that GPC can potentiate the mitochondrial activity. To further clarify this issue, another protocol was applied by adding substrates and inhibitors of individual ETC complexes. In response to complex I inhibitor rotenone, the oxygen consumption diminished significantly, which suggests that complex I is the target site of the GPC-mediated action.

We have investigated IR-induced ETC changes together with XOR and NADPH oxidases responses. The activity of both pro-inflammatory enzymes were decreased in response to GPC administration, which suggests that its primary influence on leak respiration was followed by secondary consequences on the main extra-mitochondrial, i.e. cellular enzymes involved in ROS formation. Furthermore, the IR-induced increases in superoxide and H_2O_2 levels in the circulating blood were accompanied by increased local NOx concentrations, providing indirect evidence for an evolving oxido-nitrosative stress in the liver tissue. RNS acting together with ROS generates “footprints” of tissue damage

(Iovine 2008). ROS interacting with NO produces peroxynitrite (Knight 2002), and the nitration of mitochondrial proteins result in acute and chronic liver diseases.

In our model, the increase in MDA and other oxidative and nitrosative stress markers were significantly reduced by GPC supplementation. The need of restoration of cellular GSH levels for efficient scavenging of peroxynitrite is emphasized. GPC administration reversed the IR-induced decrease in GSH level, and maintained the ratio of GSH to GSSG.

We also detected increased MPO activity as a secondary inflammatory marker, mainly secreted by active immune cells including PMNs. Again, MPO activity was decreased after the administration of GPC. All considered, these results suggest that mitochondrial alterations preceded cellular, enzymatic ROS production, and the onset of oxidative stress in liver tissue leads to PMN activation in the circulation.

6. SUMMARY OF NEW FINDINGS

- Liver IR injury is a progressive process starting from a depressed mitochondrial ETS, then the abnormal formation of ROS leads to biomembrane damage, and finally to necrotic or apoptotic cell death.

- The mitochondrial protection afforded by CH_4 inhalation involves different components under normal conditions, during ischemia and during reperfusion, similarly to the different pathomechanisms of damage.

- 2.2% CH_4 inhalation significantly influenced the IR-related disturbances of the mitochondrial ETS and mitigated the severity of subsequent damaging events. The protective potential of CH_4 was linked to reduced cytochrome c release and a reduced number of apoptotic hepatocytes.

- Exogenous GPC influences the mitochondrial oxidative metabolism, the primary source of ROS production. The direct action of GPC on mitochondrial complex I function leads to increased oxygen consumption and reduced leak respiration.

- GPC administration attenuated membrane peroxidation and the subsequent stages of tissue damage, therefore this compound might be therapeutic in IR episodes.

- In summary, both CH_4 and GPC treatments could effectively attenuate pro-inflammatory activation in IR stress through targeting the mitochondrial oxidative metabolism.

7. ACKNOWLEDGMENTS

I express my special appreciation to Professor Mihály Boros for furthering my scientific career and for encouraging my research in the Institute of Surgical Research under his valuable scientific guidance and with his help.

I am indebted to Dr. Petra Hartmann, who helped me acquire basic experimental skills and granted me unlimited daily assistance in performing the studies and writing publications.

I am also grateful to Dr. Eszter Tuboly, who guided my research work in the high-resolution respirometric analysis.

I thank all the technicians at the Institute of Surgical Research for providing a stable background for the experiments and the biochemical assays.

Last but not least, I would like to acknowledge the part played by my family for their continuous belief and support.

This thesis was supported by (OTKA) K104656, NKFI K120232 grants and GINOP-2.3.2-15-2016-00015.

8. REFERENCES

Abbiati G, Fossati T, Lachmann G, Bergamaschi M, Castiglioni C. Absorption, tissue distribution and excretion of radiolabelled compounds in rats after administration of [14C]-L-alpha-glycerylphosphorylcholine. Eur J Drug Metab Pharmacokinet. 1993;18:173-80.

Acín-Pérez R, Bayona-Bafaluy MP, Fernández-Silva P, Moreno-Loshuertos R, Pérez-Martos A, Bruno C, Moraes CT, Enríquez JA. Respiratory complex III is required to maintain complex I in mammalian mitochondria. Mol Cell. 2004;13:805-15.

Alberts B, Johnson A, Lewis J, Raff M, Roberts K, Walter P. Molecular Biology of the Cell. New York: Garland Publishing Inc. 1994.

Alpini G, Glaser SS, Ueno Y, Rodgers R, Phinizy JL, Francis H, Baiocchi L, Holcomb LA, Caligiuri A, LeSage GD. Bile acid feeding induces cholangiocyte proliferation and secretion: evidence for bile acid-regulated ductal secretion. Gastroenterology. 1999;116:179-86.

Althoff F, Jugold A, Keppler F. Methane formation by oxidation of ascorbic acid using iron minerals and hydrogen peroxide. Chemosphere. 2010;80:286-92.

Anderson EJ, Katunga LA, Willis MS. Mitochondria as a source and target of lipid peroxidation products in healthy and diseased heart. Clin Exp Pharmacol Physiol. 2012;39:179-93.

Aon MA, Cortassa S, O'Rourke B. Redox-optimized ROS balance: a unifying hypothesis. Biochim Biophys Acta. 2010;1797:865-77.

Attaluri A, Jackson M, Valestin J, Rao SS. Methanogenic flora is associated with altered colonic transit but not stool characteristics in constipation without IBS. Am J Gastroenterol. 2010;105:1407-11.

Beckman JS, Parks DA, Pearson JD, Marshall PA, Freeman BA. A sensitive fluorometric assay for measuring xanthine dehydrogenase and oxidase in tissues. Free Radic Biol Med. 1989;6:607-15.

Bencsik P, Kupai K, Giricz Z, Görbe A, Pipis J, Murlasits Z, Kocsis GF, Varga-Orvos Z, Puskás LG, Csonka C, Csont T, Ferdinandy P. Role of iNOS and peroxynitrite-matrix metalloproteinase-2 signaling in myocardial late preconditioning in rats. Am J Physiol Heart Circ Physiol. 2010;299:H512-H518.

Bevan C, Kinne RK. Choline transport in collecting duct cells isolated from the rat renal inner medulla. Pflugers Arch. 1990;417:324-8.

Bianchi C, Genova ML, Parenti Castelli G, Lenaz G. The mitochondrial respiratory chain is partially organized in a supercomplex assembly: kinetic evidence using flux control analysis. J Biol Chem. 2004;279:36562-9.

Boros M, Ghyczy M, Erces D, Varga G, Tokes T, Kupai K, Torday C, Kaszaki J. The anti-inflammatory effects of CH_4. Crit Care Med. 2012;40:1269-78.

Boros M, Wolfárd A, Ghyczy M. In vivo evidence of reductive stress-induced CH_4 production. Shock. 1999;12:56.

Boumans H, Grivell LA, Berden JA. The respiratory chain in yeast behaves as a single functional unit. J Biol Chem. 1998;273:4872-7.

Brownawell AM, Carmines EL, Montesano F. Safety assessment of AGPC as a food ingredient. Food Chem Toxicol. 2011;49:1303-15.

Bruhl A,Hafner G, Loffelholz K. Release of choline in the isolated heart, an indicator of ischemic phospholipid degradation and its protection by ischemic preconditioning: no evidence for a role of phospholipase D. Life Sci. 2004;75:1609-20.

Caldwell SH, Swerdlow RH, Khan EM, Iezzoni JC, Hespenheide EE, Parks JK, Parker WD Jr. Mitochondrial abnormalities in non-alcoholic steatohepatitis. J Hepatol. 1999;31:430-4.

Cantrell CA, Shetter RE, McDaniel AH, Calvert JG, Davidson JA, Lowe DC, Tyler SC, Cicerone RJ, Greenberg JP. Carbon kinetic isotope effect in the oxidation of methane by the hydroxyl radical. Journal of Geophysical Research: Atmospheres. 1990; 95:22455-62.

Carlisle SM, Burchart PA, McCauley C, Surette RA. Biokinetics of inhaled radioactive CH_4 in rats: a pilot study. Appl Radiat Isot. 2005;62:847-60.

Chang CJ, Yin PH, Yang DM, Wang CH, Hung WY, Chi CW, Wei YH, Lee HC. Mitochondrial dysfunction-induced amphiregulin upregulation mediates chemo-resistance and cell migration in HepG2 cells. Cell Mol Life Sci. 2009;66:1755–65.

Chen O, Ye Z, Cao Z, Manaenko A, Ning K, Zhai X, Zhang R, Zhang T, Chen X, Liu W, Sun X. Methane attenuates myocardial ischemia injury in rats through anti-oxidative, anti-apoptotic and anti-inflammatory actions. Free Radic Biol Med. 2016;90:1-11.

Clark JM, Brancati FL, Diehl AM. Nonalcoholic fatty liver disease. Gastroenterology. 2002;122:1649-57.

Cole NB, Daniels MP, Levine RL, Kim G. Oxidative stress causes reversible changes in mitochondrial permeability and structure. Exp Gerontol. 2010;45:596-602.

De Jesus Moreno Moreno M**.** Cognitive improvement in mild to moderate Alzheimer's dementia after treatment with the acetylcholine precursor choline alfoscerate: a multicenter,

double-blind, randomized, placebo-controlled trial. Clin Ther. 2003;25:178-93.

Denman SE, Tomkins NW, McSweeney CS. Quantitation and diversity analysis of ruminal methanogenic populations in response to the antimethanogenic compound bromochloromethane. FEMS Microbiol Ecol. 2007; 62:313-22.

Diaz F, Fukui H, Garcia S, Moraes CT. Cytochrome c oxidase is required for the assembly/stability of respiratory complex I in mouse fibroblasts. Mol Cell Biol. 2006;26:4872-81.

Domenis R, Comelli M, Bisetto E, Mavelli I. Mitochondrial bioenergetic profile and responses to metabolic inhibition in human hepatocarcinoma cell lines with distinct differentiation characteristics. J Bioenerg Biomembr. 2011;5:493-505.

Domenis R, Comelli M, Bisetto E, Mavelli I. Mitochondrial bioenergetic profile and responses to metabolic inhibition in human hepatocarcinoma cell lines with distinct differentiation characteristics. J Bioenerg Biomembr. 2011;43:493-505.

Dougherty RW, O'Toole JJ, Allison MJ. Oxidation of intra-arterially administered carbon 14-labelled methane in sheep. Proc Soc Exp Biol Med. 1967;124:1155-7.

Farber SA, Slack BE, Blusztajn JK. Acceleration of phosphatidylcholine synthesis and breakdown by inhibitors of mitochondrial function in neuronal cells: a model of the membrane defect of Alzheimer's disease. FASEB J. 2000;14:2198-206.

Farooqui AA, Yang HC, Rosenberger TA, Horrocks LA. Phospholipase A2 and its role in brain tissue. J Neurochem. 1997;69:889-901.

Ferdinandy P, Danial H, Ambrus I, Rothery RA, Schulz R. Peroxynitrite is a major contributor to cytokine-induced myocardial contractile failure. Circ Res. 2000;87:241-7.

Ghyczy M, Torday C, Kaszaki J, Szabó A, Czóbel M, Boros M. Hypoxia-induced generation of CH_4 in mitochondria and eukaryotic cells: an alternative approach to methanogenesis. Cell Physiol Biochem. 2008;21:251-58.

Ghyczy M, Torday C, Kaszaki J, Szabó A, Czóbel M, Boros M. Oral phosphatidylcholine pretreatment decreases ischemia-reperfusion-induced methane generation and the inflammatory response in the small intestine. Shock. 2008;30:596-602.

Gibellini F, Smith TK. The Kennedy pathway--De novo synthesis of phosphatidylethanolamine and phosphatidylcholine. IUBMB Life. 2010;62:414-28.

Gnaiger E, Kuznetsov AV, Schneeberger S, Seiler R, Brandacher G, Steurer W, Margreiter R. Mitochondria in the cold. In: Life in the Cold. New York: Springer, 2000:431-442.

Gnaiger E.Bioenergetics at low oxygen: dependence of respiration and phosphorylation on

oxygen and adenosine diphosphate supply. Respir Physiol. 2001;128:277-97.

Goetz M, Ansems JV, Galle PR, Schuchmann M, Kiesslich R. In vivo real-time imaging of the liver with confocal endomicroscopy permits visualization of the temporospatial patterns of hepatocyte apoptosis. Am J Physiol Gastrointest Liver Physiol. 2011;301:764-72.

Granger DN, Höllwarth ME, Parks DA. Ischemia-reperfusion injury: role of oxygen-derived free radicals. Acta Physiol Scand Suppl. 1986;548:47-63.

Hamilton JT, McRoberts WC, Keppler F, Kalin RM, Harper DB. (2003). Chloride methylation by plant pectin: an efficient environmentally significant process. Science. 2003;301:206–9.

Hartmann P, Fet N, Garab D, Szabó A, Kaszaki J, Srinivasan PK, Tolba RH, Boros M. L-α-glycerylphosphorylcholine reduces the microcirculatory dysfunction and nicotinamide adenine dinucleotide phosphate-oxidase type 4 induction after partial hepatic ischemia in rats. J Surg Res. 2014;189:32-40.

He R, Wang L, Zhu J, Fei M, Bao S, Meng Y, Wang Y, Li J, Deng X. Methane-rich saline protects against concanavalin A-induced autoimmune hepatitis in mice through anti-inflammatory and anti-oxidative pathways. Biochem Biophys Res Commun. 2016;470:22-8.

Heathcote EJ. Diagnosis and management of cholestatic liver disease Clin Gastroenterol Hepatol. 2007;5:776-82.

Hines IN, Hoffman JM, Scheerens H, Day BJ, Harada H, Pavlick KP, Bharwani S, Wolf R, Gao B, Flores S, McCord JM, Grisham MB. Regulation of postischemic liver injury following different durations of ischemia. Am J Physiol Gastrointest Liver Physiol. 2003;284:G536-G545.

Hirakawa A, Takeyama N, Nakatani T, Tanaka T. Mitochondrial permeability transition and cytochrome c release in ischemia-reperfusion injury of the rat liver. J Surg Res. 2003;111:240-7.

Hurkuck M, Althoff F, Jungkunst HF, Jugold A and Keppler F. Release of methane from aerobic soil: an indication of a novel chemical natural process? Chemosphere. 2012; 86:684-9.

Hutter E, Skovbro M., Lener B., Prats C., Rabol R., Dela F., Jansen-Dürr P. Oxidative stress and mitochondrial impairment can be separated from lipofuscin accumulation in aged human skeletal muscle. Aging Cell. 2007;6:245-56.

Ibdah JA, Perlegas P, Zhao Y, Angdisen J, Borgerink H, Shadoan MK, Wagner JD, Matern

D, Rinaldo P, Cline JM. Mice heterozygous for a defect in mitochondrial trifunctional protein develop hepatic steatosis and insulin resistance. Gastroenterology. 2005;128:1381-90.

Infante JP**.** De novo CDP-choline-dependent glycerophosphorylcholine synthesis and its involvement as an intermediate in phosphatidylcholine synthesis. FEBS Lett. 1987;214:149-52.

Iovine NM, Pursnani S, Voldman A, Wasserman G, Blaser MJ, Weinrauch Y. Reactive nitrogen species contribute to innate host defense against Campylobacter jejuni. Infect Immun. 2008;76:986-93.

Jelenik T, Roden M. Mitochondrial plasticity in obesity and diabetes mellitus. Antioxid Redox Signal. 2013;19:258-68.

Jelenik T, Roden M. Mitochondrial plasticity in obesity and diabetes mellitus. Antioxid Redox Signal. 2013;19:258-68.

Kalashnyk OM, Gergalova GL, Komisarenko SV, Skok MV. Intracellular localization of nicotinic acetylcholine receptors in human cell lines. Life Sci. 2012;91:1033-7.

Kenneth BS. Functional metabolism: regulation and adaptation. John Wiley&Sons Inc.; Hoboken, New Yew Jersey, 2005: 640 p

Keppler F, Boros M, Frankenberg C, Lelieveld J, McLeod A, Pirttilä AM, Röckmann T, Schnitzler JP. Methane formation in aerobic environments. Environ Chem. 2009;6:459–65.

Kiemer AK, Heinze SK, Gerwig T, Gerbes AL, Vollmar AM. Stimulation of p38 MAPK by hormonal preconditioning withatrial natriuretic peptide. World J Gastroenterol. 2002;8:707-11.

Knight TR**,** Ho YS, Farhood A, Jaeschke H. Peroxynitrite is a critical mediator of acetaminophen hepatotoxicity in murine livers: protection by glutathione. J Pharmacol. Exp Ther. 2002;303:468-75.

Krause F, Reifschneider NH, Goto S, Dencher NA. Active oligomeric ATP synthases in mammalian mitochondria. Biochem Biophys Res Commun. 2005;329:583-90.

Kuebler WM, Abels C, Schuerer L, Goetz AE. Measurement of neutrophil content in brain and lung tissue by a modified myeloperoxidase assay. Int J Microcirc Clin Exp. 1996;16:89-97.

Lei DX, Peng CH, Peng SY, Jiang XC, Wu YL, Shen HW. Safe upper limit of intermittent hepatic inflow occlusion for liver resection in cirrhotic rats. World J Gastroenterol. 2001;7:713-7.

Lenaz G**,** Genova ML. Structural and functional organization of the mitochondrial respiratory chain: a dynamic super-assembly. Int J Biochem Cell Biol. 2009;41:1750-72.

Lesnefsky EJ, Moghaddas S, Tandler B, Kerner J, Hoppel CL. Mitochondrial dysfunction in cardiac disease: ischemia--reperfusion, aging, and heart failure. J Mol Cell Cardiol. 2001;33:1065-89.

Levine RL, Mosoni L, Berlett BS, Stadtman ER. Methionine residues as endogenous antioxidants in proteins. Proc Natl Acad Sci USA. 1996;93:15036-40.

Levitt MD, Furne JK, Kuskowski M, Ruddy J. Stability of human methanogenic flora over 35 years and a review of insights obtained from breath methane measurements. Clin Gastroenterol Hepatol. 2006;4:123-9.

Li MK, Crawford JM. The pathology of cholestasis. Semin Liver Dis. 2004;24:21-42.

Li Z, Graham BH. Measurement of mitochondrial oxygen consumption using a Clark electrode. Methods Mol Biol. 2012;837:63-72.

Liu Y, Luo HS, Liang CB, Tan W, Xia H, Xu WJ. Effects of methane on proximal colon motility of rats and ion channel mechanisms [Article in Chinese]. Zhonghua Yi Xue Za Zhi. 2013;93:459-63.

Lojek A, Milancíz, Slavíková H, Dusková M, Vondrácek J, Kubala L, Rácz I, Hamar J. Leukocyte mobilization, chemiluminescence response, and antioxidative capacity of the blood in intestinal ischemia and reperfusion. Free Radic Res. 1997;27:359-67.

McCord JM. Oxygen-derived free radicals in postischemic tissue injury. N Engl J Med. 1985;312:159-63.

Meyer M, Tebbe U, Piiper J. Solubility of inert gases in dog blood and skeletal muscle. Pflugers Arch. 1980;384:131-4.

Mitchell L, Brook E, Lee JE, Buizert C, Sowers T. Constraints on the late holocene anthropogenic contribution to the atmospheric methane budget. Science. 2013;342:964-6.

Parnetti L, Amenta F, Gallai V. Choline alphoscerate in cognitive decline and in acute cerebrovascular disease: an analysis of published clinical data. Mech Ageing Dev. 2001;122:2041-55.

Pessayre D, Fromenty B. NASH: a mitochondrial disease. J Hepatol. 2005; 42:928-40.

Pfeiffer K**,** Gohil V, Stuart RA, Hunte C, Brandt U, Greenberg ML, Schägger H. Cardiolipin stabilizes respiratory chain supercomplexes. J Biol Chem. 2003;278:52873-80.

Phielix E, Szendroedi J, Roden M. Mitochondrial function and insulin resistance during aging: a mini-review. Gerontology. 2011;57:387-96.

Picard M, Taivassalo T, Ritchie D, Wright KJ, Thomas MM, Romestaing C, Hepple RT. Mitochondrial structure and function are disrupted by standard isolation methods. PLoS One. 2011;6:e18317.

Pimentel M, Chang C, Chua KS, Mirocha J, DiBaise J, Rao S, Amichai M. Antibiotic treatment of constipation-predominant irritable bowel syndrome. Dig Dis Sci. 2014;59:1278-85.

Pimentel M, Lin HC, Enayati P, van den Burg B, Lee HR, Chen JH, Park S, Kong Y, Conklin J. Methane, a gas produced by enteric bacteria, slows intestinal transit and augments small intestinal contractile activity. Am J Physiol Gastrointest Liver Physiol. 2006;290:G1089-95.

Placer ZA, Cusman L, Johnson B.C. Estimation of product of lipid peroxidation by malonyldialdehyde in biochemical systems. Anal Biochem. 1966;16:359-64.

Purnak T, Beyazit Y, Ibis M, Koklu S, Efe C, Ozaslan E, Ciftci A, Tenlik I. The involvement of nitric oxide in the physiopathology of hepatoportal sclerosis. Clin Biochem. 2012;45:1450-4.

Roccarina D, Lauritano EC, Gabrielli M, Franceschi F, OjettiV, Gasbarrini A. The role of methane in intestinal diseases. Am J Gastroenterol. 2010;105:1250-6.

Rose S, Frye RE, Slattery J, Wynne R, Tippett M, Melnyk S, James SJ. Oxidative stress induces mitochondrial dysfunction in a subset of autistic lymphoblastoid cell lines. Transl Psychiatry. 2014;4:e377.

Sanyal AJ, Campbell-Sargent C, Mirshahi F, Rizzo WB, Contos MJ, Sterling RK, Luketic VA, Shiffman ML, Clore JN. Nonalcoholic steatohepatitis: association of insulin resistance and mitochondrial abnormalities. Gastroenterology. 2001;120:1183-92.

Scapicchio PL**.** Revisiting choline alphoscerate profile: a new, perspective, role in dementia? Int J Neurosci. 2013;123:444-9.

Schoenberg MH, Poch B, Younes M, Schwarz A, Baczako K, Lundberg C, Haglund U, Beger HG. Involvement of neutrophils in postischaemic damage to the small intestine. Gut. 1991;32:905-12.

Schöttl T, Kappler L, Braun K, Fromme T, Klingenspor M. Limited mitochondrial capacity of visceral versus subcutaneous white adipocytes in male C57BL/6N mice. Endocrinology. 2015;156:923-33.

Schöttl T, Kappler L, Fromme T, Klingenspor M. Limited OXPHOS capacity in white adipocytes is a hallmark of obesity in laboratory mice irrespective of the glucose tolerance

status. Mol Metab. 2015;4:631-42.

Scribner DM, Witowski NE, Mulier KE, Lusczek ER, Wasiluk KR, Beilman GJ. Liver metabolomic changes identify biochemical pathways in hemorrhagic shock. J Surg Res. 2010;164:e131-e139.

Sigala S**,** Imperato A, Rizzonelli P, Casolini P, Missale C, Spano P. L-alpha-glycerylphosphorylcholine antagonizes scopolamine-induced amnesia and enhances hippocampal cholinergic transmission in the rat. Eur J Pharmacol. 1992;211:351-8.

Song K, Zhang M, Hu J, Liu Y, Liu Y, Wang Y, Ma X. Methane-rich saline attenuates ischemia/reperfusion injury of abdominal skin flaps in rats via regulating apoptosis level. BMC Surg. 2015;15: 1-8.

Szarka A, Horemans N, Banhegyi G, Asard H. Facilitated glucose and dehydroascorbate transport in plant mitochondria. Arch Biochem Biophys. 2004;428:73-80.

Tahara EB, Navarete FD, Kowaltowski AJ. Tissue-, substrate-, and site-specific characteristics of mitochondrial reactive oxygen species generation. Free Radic Biol Med. 2009; 9:1283–97.

Tőkés T, Tuboly E, Varga G, Major L, Ghyczy M, Kaszaki J, Boros M. Protective effects of L-alpha-glycerylphosphorylcholine on ischaemia-reperfusion-induced inflammatory reactions. Eur J Nutr. 2015;54:109-18.

Traini E, Bramanti V, Amenta F. Choline alphoscerate (alpha-glyceryl-phosphoryl-choline) an old choline- containing phospholipid with a still interesting profile as cognition enhancing agent. Curr Alzheimer Res. 2013;10:1070-9.

Tuboly E, Szabó A, Garab D, Bartha G, Janovszky Á, Erős G, Szabó A, Mohácsi Á, Szabó G, Kaszaki J, Ghyczy M, Boros M. CH_4 biogenesis during sodium azide-induced chemical hypoxia in rats. Am J Physiol Cell Physiol. 2013;304:C207-14.

Wang X. The expanding role of mitochondria in apoptosis. Genes Dev. 2001;15:2922-33.

Wei Y, Rector RS, Thyfault JP, Ibdah JA. Nonalcoholic fatty liver disease and mitochondrial dysfunction. World J Gastroenterol. 2008;14:193-9.

Weissbach H, Resnick L, Brot N. Methionine sulfoxidereductases: history and cellular role in protecting against oxidative damage. Biochim Biophys Acta. 2005;1703:203-12.

Wu J, Wang R, Ye Z, Sun X, Chen Z, Xia F, Sun Q, Liu L. Protective effects of methane-rich saline on diabetic retinopathy via anti-inflammation in a streptozotocin-induced diabetic rat model. Biochem Biophys Res Commun. 2015;466:155-61.

Ye Z, Chen O, Zhang R, Nakao A, Fan D, Zhang T, Gu Z, Tao H, Sun X. Methane

attenuates hepatic ischemia/reperfusion injury in rats through antiapoptotic, anti-inflammatory, and antioxidative actions. Shock. 2015;44:181-7.

Zablocki K, Miller SP, Garcia-Perez A, Burg MB. Accumulation of glycerophosphocholine (GPC) by renal cells: osmotic regulation of GPC: choline phosphodiesterase. Proc Natl Acad Sci U S A. 1991;88:7820-4.

Zhang M, Mileykovskaya E, Dowhan W. Gluing the respiratory chain together. Cardiolipin is required for supercomplex formation in the inner mitochondrial membrane. J Biol Chem. 2002;277:43553-6.

9. ANNEX